NTNU
Norwegian University of
Science and Technology

Design of a Test Rig for Investigations of Flow Transient

Lise Rikstad

Mechanical Engineering
Submission date: June 2016
Supervisor: Pål Tore Selbo Storli, EPT

Norwegian University of Science and Technology
Department of Energy and Process Engineering

NTNU
Norwegian University
of Science and Technology

Department of Energy
and Process Engineering

EPT-M-2016-103

MASTER THESIS

for

Student
Lise Rikstad

Spring 2016

Design of a test rig for investigations of flow transient

Design av en testrig for undersøkelse av transienter i strømning

Background and objective

The dynamic nature of the electrical energy system leads to changes in the operating point of a hydraulic turbine, where both energy production and rotational speed changes. This causes the conditions in the tunnels and conduits of hydro power plants to rarely be stationary, there is always some dynamics in the water system. The friction losses in the unsteady flow is not well described, and for this reason a test rig is intended established at the Waterpower lab.

The objective of the master thesis will be to establish the design of the test rig such that it is possible to perform measurements for the evaluation of the friction involved in the problem.

The following tasks are to be considered:

1. Literature study on the dynamics of closed conduit flow, both 1D and 3D for large scale properties as well as details in unsteady flow
2. Identification of measurement techniques that allow for measurements with high spatial and temporal resolution
3. Consider existing laboratory limitations and identify which dynamic situations it is possible to test and perform measurements on for a future rig at the Waterpower laboratory.
4. Suggest and specify the final design of the rig which allow for flexible and easy operation and which facilitates the desired measurements
5. Suggest and specify the instrumentation needed on the rig to be able to perform the desired measurements.

-- " --

Within 14 days of receiving the written text on the master thesis, the candidate shall submit a research plan for his project to the department.

When the thesis is evaluated, emphasis is put on processing of the results, and that they are presented in tabular and/or graphic form in a clear manner, and that they are analyzed carefully.

The thesis should be formulated as a research report with summary both in English and Norwegian, conclusion, literature references, table of contents etc. During the preparation of the text, the candidate should make an effort to produce a well-structured and easily readable report. In order to ease the evaluation of the thesis, it is important that the cross-references are correct. In the making of the report, strong emphasis should be placed on both a thorough discussion of the results and an orderly presentation.

The candidate is requested to initiate and keep close contact with his/her academic supervisor(s) throughout the working period. The candidate must follow the rules and regulations of NTNU as well as passive directions given by the Department of Energy and Process Engineering.

Risk assessment of the candidate's work shall be carried out according to the department's procedures. The risk assessment must be documented and included as part of the final report. Events related to the candidate's work adversely affecting the health, safety or security, must be documented and included as part of the final report. If the documentation on risk assessment represents a large number of pages, the full version is to be submitted electronically to the supervisor and an excerpt is included in the report.

Pursuant to "Regulations concerning the supplementary provisions to the technology study program/Master of Science" at NTNU §20, the Department reserves the permission to utilize all the results and data for teaching and research purposes as well as in future publications.

The final report is to be submitted digitally in DAIM. An executive summary of the thesis including title, student's name, supervisor's name, year, department name, and NTNU's logo and name, shall be submitted to the department as a separate pdf file. Based on an agreement with the supervisor, the final report and other material and documents may be given to the supervisor in digital format.

☒ Work to be done in lab (Water power lab, Fluids engineering lab, Thermal engineering lab)
☐ Field work

Department of Energy and Process Engineering, 13. January 2016

Olav Bolland
Department Head

Pål-Tore Storli
Academic Supervisor

Research Advisor:
Torbjørn Nielsen

Abstract

Frictional losses during unsteady flow in the waterway of power plants are a progressing science, as the hydropower market keeps evolving to a more dynamic market. In fact, the transitional region in pipe flow is a rather unknown phenomenon. The experimental data on the topic is limited and there are no analytical solutions.

This study looks into the opportunity of establishing a test rig to study frictional losses in oscillating pipe flow, at the Water Power Laboratory at the Norwegian University of Science and Technology (NTNU). Previous work on oscillating pipe flow mainly addresses flow in U-tubes. There are only a few experimental test rigs for oscillations in horizontal pipes, which primarily generates oscillations by the use of pistons. In this thesis, a different approach applies: the shutdown of a control valve generates oscillations in a horizontal pipe between a surge shaft and a reservoir.

The study is a combination of relevant measuring techniques, laboratory considerations and applicable instrumentation to design a flexible and easy operated test rig. A review of the basic theory of transient pipe flow is the first part of this thesis. The second part presents relevant pressure transducers and connections for measuring head loss in pipe flow. Followed by measuring techniques to measure local velocities: Particle Image velocimetry, Laser Doppler Anemometer and Hot-Wire Anemometer.

An important part of the study was to consider the limitations and constraints in the Water Power Laboratory. A thorough review of the laboratory was therefore necessary. The final part presents the required apparatuses and devices to create the desired flow through the test section, including challenges and alternatives to solution.

The results describe the flow situations that are possible to obtain in The Water Power Laboratory. Followed by descriptions of recommended apparatuses and necessary instrumentations. At last, an overview of measuring techniques recommended for specific fields of interest is presented.

Sammendrag

Kraftbransjen utvikler seg stadig mot et mer dynamisk marked. Denne utviklingen øker behovet for kunnskap om friksjonstap i ikke-stasjonær strømning i vannveien av vannkraftanlegg. Transiente strømningsfenomener er relativt ukjente. Det er begrenset med eksperimentell data om denne type strømning og per i dag finnes det ingen analytiske løsninger.

Denne oppgaven tar for seg muligheten for å etablere en testrigg for undersøkelse av friksjonstap i ikke-stasjonær strømning ved Vannkraftlaboratoriet på NTNU. Tidligere studier på massesvingninger retter seg i hovedsak mot svingninger i U-rør. Det er kun et fåtall testrigger som har studert massesvingninger i horisontale rør. I de fleste tilfellene er svingningene her produsert av et stempel. I denne oppgaven genereres svingningene, mellom et reservoar og en svingesjakt, ved hurtig lukking av en ventil.

Denne oppgaven tar utgangspunkt i relevante målemetoder, begrensninger gitt av laboratoriet og egnet instrumentering for å designe en fleksibel test rigg. En gjennomgang av den grunnleggende teorien bak transiente rørstrømning er gitt i første del av oppgaven. Andre del presenterer relevante trykksensorer og koblingsmetoder for å måle trykktap langs røret. Etterfulgt av målemetoder for å måle lokale hastigheter: Particle Image velocimetry, Laser Doppler Anemometer and Hot-Wire Anemometer.

En viktig del av oppgaven var å vurdere begrensninger og restriksjoner i vannkraftlaboratorier. En nøye gjennomgang av laboratoriet var derfor nødvendig. Den siste delen av oppgaven presentere det nødvendige utstyret og instrumentene for å skape den ønskede strømningen i testseksjonen. Dette kapittelet tar også for seg utfordringer og alternativer til løsninger.

Resultatet beskriver hvilke dynamiske strømninger det er mulig å oppnå i Vannkraftlaboratoriet. Etterfulgt av anbefalt utstyr og nødvendig instrumentering. Tilslutt er det presentert en oversikt over hvilke målemetode som er anbefalt for hvert spesifikke undersøkelsesområde.

Preface

The following master´s thesis is written during the spring semester of 2016 at the Norwegian University of Science and Technology (NTNU). This thesis concludes my Master studies of Mechanical Engineering, Department of Energy and Process Engineering. I started my engineering studies inspired by the need of renewable energy and I feel lucky to end my studies in the interesting and renewable field of hydropower.

I wanted a multidisciplinary and practical thesis to test my theoretical knowledge, and I was therefore delighted when I got the chance to project a test rig for the Water Power Laboratory.

I have truly appreciated being a part of the unique social and working environment at the Water Power Laboratory. I would like to thank PhD student, Peter Joachim Gogstad, for interesting discussions and help along the way. Finally, I would like to thank my supervisor, Pål-Tore Storli.

Trondheim, 08.06.2016

Lise Rikstad

Table of Contents

List of Figures

List of Tables

List of Symbols

Symbol	Unit	Description
A	m^2	Area
A_s	m^2	Area surge shaft
A_t	m^2	Area waterway
a	m/s	Absolute velocity
c	m/s	Absolute velocity
C_d	-	Discharge coefficient
D	m	Diameter
D_h	m	Hydraulic Diameter
d	m	Diameter
e	mm	Roughness
f	-	Friction factor
f	Hz	Frequency
f_s	Hz	Sampling frequency
g	m/s^2	Gravitational acceleration
H	MWC	Pressure height
h_f	MWC	Head loss
h_L	MWC	Head loss
k	-	Loss coefficient
L	m	Length
P	N/m^2	Pressure
p	N/m^2	Pressure
P_L	N/m^2	Pressure loss
Q	m^3/s , l/s	Flow rate
R_s	m	Spillway crest radius
t	s	Time
T	s	Period
u	m/s	Velocity
V	m/s	Velocity
v	m/s	Velocity
V_0	m/s	Steady state velocity
x, y, z		Coordinates

Symbol	Unit	Description
μ	kg/(m•s)	Dynamic viscosity
ρ	kg/m^3	Mass density
ζ	-	Local loss coefficient
θ	°	Angle
v	m^2/s	Kinematic viscosity
ω	Rad/s	Angular frequency

1 Introduction

1.1 Background

On a global basis, hydropower stands for one-sixth of the world's power production. Hydropower plants are highly reliable and flexible; no other renewable energy source can match its capabilities. In recent years, the development of other renewable energy sources has changed the electrical system. Most renewable energy sources, as wind and solar power, are weather dependent, which makes them unreliable. This development increases the need of an energy sources to stabilize the grid. The reservoir capacity and regulation abilities of hydropower plants makes hydropower an essential part and contributor to today's energy system.

Historically, hydropower plants were designed for operating at best efficiency point and with minor changes in water discharge and power output. In recent years, this operating regime has changed to become more dynamic, where the power output is constantly adjusted. Operating at part load and with sudden starts and stops can cause high pressure pulsations, known as water hammer. Surge shafts are implemented in hydropower plants where there is a risk of damaging pressure pulsations. Surge shafts are necessary to limit the retardation pressure in front of the turbine. It also improves the plants regulation ability. Surge shafts are located between the reservoir and the turbine, to reduce the distance to the nearest free surface. Surge shafts are a solution to the problem of water hammer; however, they introduce the problem of mass oscillations between the surge shaft and the reservoir.

The development of a more dynamic electrical market leads to constantly varying flow in the tunnels and penstocks of hydropower plants. The friction losses during unsteady flow are not certain; research are therefore necessary to increase the knowledge to enhance the operational efficiency of hydropower plants.

Fluid flows are highly complex, which makes theoretical analyses time consuming. In fact, theoretical analyses are often unable to reach a solution for specific flows, including transient flow. Nowadays, the method of computational fluid dynamics (CFD) is a wide application in the study of fluid flows. CFD uses numerical analysis and algorithms to solve and analyse problems in fluid flows. However, this does not compensate for experimental study, but rather

makes experimental validation even more important to enhance the general reliability and applicability of CFD.

1.2 Problems to be addressed

This thesis is the first step towards the establishment of a test rig for investigation of frictional losses in oscillating pipe flow. The test rig is intended established at the Water Power Laboratory at the Norwegian University of Science and Technology (NTNU).

The primary questions to investigate are; firstly, which flow situations are possible to obtain given the laboratory limitations? Secondly, what measurement techniques are applicable for the investigation of frictional losses in oscillating pipe flow? Thirdly, how should the design of the test rig be to create the desired flow situation? Lastly, what instruments and devices are required to perform the desired measurements?

In order to address these questions, it is necessary with a review of the relevant measuring techniques, the Water Power Laboratory and applicable apparatus, devices and instruments.

1.3 Framework

The establishment of such a test rig has been a desire for several years at the Water Power Laboratory, and has led to the purchase of a few components intended for the test rig. These components must be considered throughout the evaluation process.

The laboratory has various test loops and equipment, which limits the adequate space and the availability to construct the test rig.

The purchase of the remaining parts and devices are dependent on sufficient funding. As of today, the project does not have funding and an anticipated budget has not been compiled. Cost accounting is not a part of this scope. However, there is a desire to establish the test rig in near future; the focus has therefore been to limit the cost of the project.

These factors form the framework, and must be combined to reach the best possible result.

1.4 Structure of the thesis

The thesis starts with a literature review on research conducted on oscillating pipe flow, as well as test rigs and models that are made for collecting experimental data on the subject. The next section is a theory chapter. This chapter review the governing equations for pipe flow, basic theory related to transients and presents the Euler Integration method. The following chapter addresses relevant measuring techniques for pipe flow; including, pressure measurements, mean velocity measurements and local velocity measurements.

The Water Power Laboratory chapter includes three sections. The first one states the relevant infrastructure and constraints of the laboratory. The second and third section gives a description of the available and purchased components for the test rig.

The following chapter describes the apparatus, devices and instruments needed to form a test rig and to produce and measure the desired flow.

The result and discussion chapter systematically presents suggestions of the test rig design and recommended measurement techniques. A discussion follows the sub-chapters. Whereas the conclusion chapter summarize the most important finding.

2 Literature Review

The problem of oscillating flow has been studied for more than a 100 years, but because of its complexity and lack of experimental data, a thorough understanding of the phenomena has not yet been achieved.

In a historical point of view, the oscillation of liquid in a vertical U-tube was discussed in the book of Principia by Newton already in 1687. Further, Bernoulli gave out the book Hydrodynamica, where he discussed the oscillation of motion of a liquid column. His research was restricted to inviscid fluid (Bernoulli, 1968). In 1966, Sergeev and several other researchers published papers concerning the stability of Stokes boundary layers. During 1976, Hino et al. used hot wire measurements to study the transition to turbulence in an oscillating flow. Their results showed a laminar flow during acceleration phase of the half cycle and a turbulent flow during the deceleration phase (1976). By flow visualization, Sergeev found the correlation equation for predicting the transition to turbulence flow.

Later on, Manneret derived the fundamental solution of the damped oscillation of the viscous liquid column in the vertical u-tube (Iguchi, Ohmi and Maegawa, 1982). Both Sawanoto-Hino and Yasukawa – Tagawa analyzed free oscillating turbulent flow. In 1982 Iguchi, Ohmi and Maegawa studied the fact that a free oscillating turbulent flow is not turbulent over one cycle, but it consists of the preceding laminar and subsequent turbulent phases. They stated that a free oscillating flow in a U-shaped tube could be divided into three categories, i.e. laminar, transitional and turbulent flow. Their experimental set up consisted of a piston-cylinder in a horizontal pipe that worked as the test section. Two pressure transducers of semiconductor type, connected to a dynamic strain meter, were applied to measure the pressure drop (Iguchi, Ohmi and Maegawa, 1982).

Another experiment was carried out where the oscillating flow was generated by a piston-crank mechanism. The variation range of the oscillation frequency was here 0.0527 – 6.24 Hz and the Reynolds number had a maximum value of 10^5. Velocity measurements were made by using a hot wire anemometer (Ohmi, 1982).

In 1983, S.W.TU and B.R. Ramaprian made an experiment on fully developed periodic turbulent pipe flow. They used static pressure taps and an inverted U-tube water manometer. Instantaneous velocity measurements in the axial direction were measured using frequency – shifted laser Doppler anemometry.

Seume (1988) experimentally studied the transition in an oscillatory pipe flow using hot film anemometry measurements. He based the experiment on parameters range covered in the heat exchanger of Stirling engines and cryocoolers.

Lodahl, Sumer and Fredsøe (1998) studied experimentally the oscillatory flow in a circular pipe. Their experiments were carried out in a 10-meter water tunnel. The flow rate was measured using a magnetic flow meter and a two-component Laser Doppler anemometer. Similar to the results of Hino, Sawamoto and Takasu (1976) and other researchers, they (Lodahl, Sumer and Fredsøe, 1998) also noted high turbulence in the decelerating phase.

M.Eckmann and B. Grotberg (1990) applied a Laser-Doppler velocimetry to conduct measurements on the transition to turbulence in oscillatory pipe flow of a Newtonian viscous fluid. In their experimental set up, they applied a piston in a vertical tube. They captured among 100 data points per cycle.

He and Jackson (2000) made a detailed investigation of turbulence under conditions of transient flow in a pipe. They applied a three-beam, two-component laser Doppler anemometer (LDA) to make measurement of local velocity components. They could measure either axial and radial, or axial and circumferential components. The LDA had a forward scatter mode of operation. Their test section also had five pressure transducers at equal intervals along the test section. The pressure differences were measured using a differential pressure transducer of capacitance type. They concluded with an uncertainty of 10% for the mean velocity measurement. The maximum uncertainty in the measurements of turbulence quantities were estimated to be about 20%. The highest sampling rate with this arrangement was approximately 15 kHz.

Doorne and Westerweel (2007) applied stereoscopic particle image velocimetry to measure the instantaneous three-component velocity field of pipe flow. When they investigated the transitional region, the time-resolved measurements were made at 62.5 Hz. They applied Taylor´s hypothesis to recover the quasi-instantaneous 3D flow field from a time-resolved measurement sequence, which was the first of its kind in pipe flow.

Researchers have shown that pipe flow can be divided into three areas. For laminar flow, analytical relationships have been developed and the results have shown very good matches with experimental data. For turbulent flow, analytically solutions are not known. However, empirical models have been developed with experimental verification. The final area is the transitional regime. The unsteady flow behaviour is unknown for the transition from laminar to turbulent or turbulent to laminar (Vítkovský, J. P., et al., 2000).

3 Theory

3.1 Hydraulic Transient in Closed Conduit

Transient flow is the intermediate-stage flow, when the conditions changes from one steady-state condition to another steady state. Transients in closed conduit flow can be divided into two types; water hammer and mass oscillation. Water hammer is a transient phenomenon that occurs in the form of traveling pressure waves. In the case of water hammer, it is important to consider the elasticity and compressibility effects. Water hammer can cause mass oscillation to occur in the waterway. If the pressure in front of the turbine is larger than what is acceptable, a surge shaft can be implemented to reduce the free surface distance from the turbine.

In penstocks, an elastic pressure wave will occur when the flow conditions changes. For instance, by regulating a valve and by starting or stopping pumps and turbines. If the penstock is short, the pressure wave will return before the valve regulation is completed, and the pressure increase will reduce. However, a long penstock will not be able to dampen the pressure wave in the same way. The pressure increase will cause great impact to the structure and will be a potential danger. There are two solutions to reduce the elastic pressure wave. First solution is to reduce the retardation of water, i.e. increase the closing time. Which is often not an alternative as there are certain requirements that have to be meet. Second solution, is to implement a free water surface close enough to the regulating valve. This decreases the hydraulic masses involved (Nilsen, 1990).

3.2 Governing Equations

The continuity and momentum equations describes the transient state flow in closed conduits. These equations are a set of partial differential equations; this is because the flow velocity and pressure in transient flow is a function of time as well as distance (Chaudhry, 1979).

This is an expression for the continuity equation:

$$\frac{\partial p}{\partial t} + V\frac{\partial p}{\partial x} + \rho a^2 \frac{\partial V}{\partial x} = 0 \tag{1}$$

The conservation of momentum is expressed with this equation:

$$\frac{\partial p}{\partial t} + V\frac{\partial V}{\partial x} + \frac{1}{\rho}\frac{\partial p}{\partial x} + g\sin\theta + \frac{fV|V|}{2D} = 0 \tag{2}$$

Equation 1 and 2 are valid for unsteady, nonuniform flow of compressible fluids in elastic conduits.

However, the governing equations can be simplified. The convective acceleration terms, $V(\partial p/\partial x)$, $V(\partial V/\partial x)$ and the slope term, $(g\sin\theta)$, are very small compared to the other terms and can therefore be neglected. In hydraulic engineering, it is common to compute pressure in terms of piezo metric head and flow rate.

For a horizontal pipe the simplified equations for continuity and momentum becomes (Chaudhry, 1979):

$$\frac{\partial H}{\partial t} + \frac{a^2}{gA}\frac{\partial Q}{\partial x} = 0 \tag{3}$$

$$\frac{\partial Q}{\partial t} + gA\frac{\partial H}{\partial x} + \frac{fQ|Q|}{2DA} = 0 \tag{4}$$

The momentum equation includes the assumption that the head losses during transient state for a given flow velocity are the same as in steady flow at the same velocity. The Darcy-Weisbach formula is included to compute the frictional losses.

3.3 Fluid Flow Regimes

The flow regime can be laminar or turbulent, or it can be transitional between the two. The flow regimes depend on the inertia to viscous forces in the stream, which is expressed with the dimensionless group, the Reynolds number. The Reynolds number for pipe flow is expressed as:

$$Re = \frac{inertial\ forces}{viscous\ forces} = \frac{\rho v D}{\mu} \tag{5}$$

Within the laminar region, the flow is stable, the stream layers move without mixing with each other and the stream flow smoothly past obstacles encountered. The turbulent region is characterized by random displacement of masses that mixes strongly with each other. For each practical installation, there is a range of critical Reynolds numbers at which defines the transition from one region to the other. For circular pipes, the critical Reynolds number is about 2300. The upper limit depends on different parameters, for instance the inlet condition and the condition of the wall surface. It is common to estimate the upper critical Reynolds number of the transitional region to be roughly 4000 (Cengel & Cimbala, 2006).

The friction factor for fully developed laminar flow in a circular pipe is a function of the Reynolds number only, as this equation shows:

$$f = \frac{64\mu}{\rho D V_{avg}} = \frac{64}{Re} \tag{6}$$

The friction factor in fully developed turbulent flow depends on the Reynolds number and the relative roughness, ε/D. The friction factor can be found either in the Moody chart or by using the implicit relation known as the Colebrook equation:

$$\frac{1}{\sqrt{f}} = -2{,}0\log\left(\frac{{}^{e}/_{D}}{3{,}7} + \frac{2{,}51}{Re\sqrt{f}}\right) \tag{7}$$

The transition from laminar to turbulent occurs over some region in which the flow fluctuates between laminar and turbulent flow. Which means that the flow may be either laminar or turbulent, or it may alternate between the two flow regimes. Thus, the friction factor may also alternate between values. The transitional flow is a very complex phenomenon, which makes the transient hydraulic problems complicated to understand (Cengel & Cimbala, 2006).

3.4 Hydrodynamic Entrance Length

When a fluid enters a circular pipe, a velocity gradient develops along the pipe. Due to the no-slip condition, the layer in contact with the wall comes to a complete stop, which causes the fluid particles in the adjacent layers to slow down gradually. This makes the fluid of the inner section of the pipe to accelerate to keep the mass flow rate constant through the pipe. The boundary layer thickness is the distance normal to the wall to a point in the flow where the flow velocity has reached the "free stream" velocity. At a certain point along the pipe the velocity becomes fully developed. The distance from the pipe inlet to the point of fully developed flow is the hydrodynamic entrance length.

Several scientists have studied the entrance length in transient pipe flow; however, a precise solution has not been obtained (Çarpinlioğlu, Özdinç, Gündoğdu, 2001). Cengel and Cimbala (2006) roughly specifies that the entry length is 115D around the critical Reynolds number (Re_{cr} = 2300).

3.5 Frictional Forces

Frictional forces in pipe flow are forces between the adjacent layers of the flowing fluid and between the fluid and the walls of the conduit. The velocity in a conduit is highest at the centre of the conduit and drops toward the wall. The wall shear stress is expressed as the tangential force per unit area that is exerted by the flowing fluid on the surface of the conduit. The magnitude of the wall shear stress is proportional to the velocity gradient near the conduit wall. The wall shear stress is much larger for turbulent flow than for laminar flow. In the core region of turbulent boundary layer, the velocity profile is changing very slowly, but very steep in the thin layer next to the wall.

The head loss, or pressure loss, is loss of energy due to friction between the fluid layers and the pipe wall, as well as local disturbances of the flow.

3.5.1 Friction Loss

This equation gives an expression of the friction loss for both laminar and turbulent flow along a straight pipe with a constant cross section (Cengel, Cimbala, 2006):

$$\Delta P_L = f \frac{L}{D} \frac{\rho v_{avg}^2}{2g} \tag{8}$$

Equation 8 is commonly expressed as head loss in terms of the equivalent fluid column height:

$$h_L = \frac{\Delta P_L}{\rho g} = f \frac{L}{D} \frac{V_{avg}^2}{2g} \tag{9}$$

3.5.2 Minor Loss

Minor pressure loss is caused by local disturbances of the flow. In a piping system, common disturbances are for instance expansions, contractions, bends and branches. All of these components contributes to the exchange of momentum between the fluid particles, thus enhancing energy dissipation. Even though these losses are referred to as minor, they might still be the largest source of loss. By having smooth transitions and rounded edges in the piping system the minor losses reduce considerably. It is recommended to place any measurement device at least 10 – 20 pipe diameters downstream of any elbows, valves or any other flow disturbance to allow the swirling turbulent eddies generated to largely disappear and the velocity profile to become fully developed.

In a general case, the local losses can be calculating using this equation (Idelchik, 1986):

$$\Delta p = \zeta \frac{p v^2}{2g} \tag{10}$$

Expressed in terms of head loss:

$$\Delta h_L = \zeta \frac{v^2}{2g} \tag{11}$$

Values for the loss coefficient can be found in the literature, for instance in Handbook of Hydraulic Resistance, Idelchik (1986). It is important to keep in mind that loss coefficients are empirical and are not valid for transient pipe flow. However, they do give an indication of what the expected losses might be.

3.6 Water Hammer

In order to explain the principle of water hammer, a simple pipeline with a reservoir and a valve downstream is illustrated along a timeline in Figure 1. Water flows from a reservoir and through a pipe with a given length. In the end of the pipe there is a valve that closes rapidly at time t = 0. At that moment, the velocity will be equal to zero upstream the valve. The kinetic energy will transform to potential energy as a pressure wave. The elastic compression that happens when the pressure increases will cause the flow to continue out of the reservoir. At the same time, the pressure wave will propagate towards the reservoir with a velocity, -c.

The pressure wave has reached the reservoir when t = L/c. The velocity in the pipeline is then zero. However, the pressure has increased throughout the pipeline. This causes the water in the pipe to start flowing back into the reservoir.

Next, the pressure front reaches back to the valve at t = 2L/c. At this moment, the pressure throughout the pipe is equal to the pressure before the valve closure. However, the water continues to flow back to the reservoir. The inertia of the water causes a negative wave to move from the valve to the reservoir with the velocity |c|. When this wave reaches the reservoir, the velocity in the pipeline is again zero. The pressure wave, that now is negative, will again reflect and move towards the valve. The water starts flowing from the reservoir to the pipe.

At t = 4 L/c the cycle is completed, but it will be repeated until all the energy is dissipated out by friction.

The time period of the pressure waves is much shorter than the mass oscillations. The pressure waves will already be dampened out when the oscillation are about to form. Which is the reason why we can threat the two phenomenon, water hammer and mass oscillation, separately (Guttormsen, 2013).

Figure 1 shows the timeline of a water hammer. From the valve closure on a steady state flow to the end of one cycle.

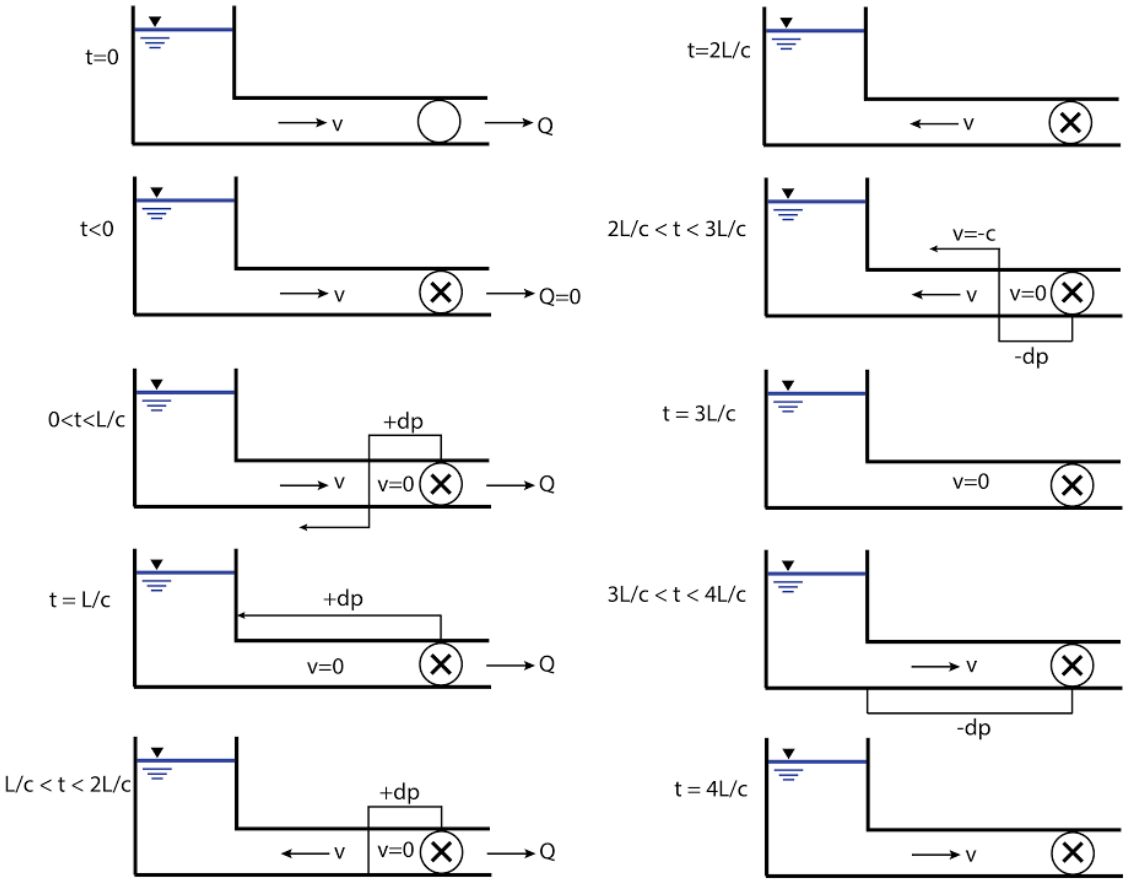

Figure 1: Water hammer pressure propagation. Based on Guttormsen (2013).

3.7 Mass Oscillation

The water hammer can reach pressure levels that are destructive to the construction and instrumentation. To avoid these pressure levels, it is common to construct a surge shaft to relieve the pressure wave. A traditional surge shaft has a free surface and it has to allow the water to exceed the hydraulic grade line in the system. Surge shafts have a variety of different designs, for instance an alternative to the traditional surge shaft is a pressurized chamber, called air cushion. Regardless of design, the reason for a surge shaft is to reduce the distance from the valve/turbine to the nearest free surface. In other words, it shortens the reflection time, which allows for fast flow regulation. A surge shaft solves the issue regarding water hammer, but it introduces a new problem; mass oscillation (Nilsen, 1990).

Figure 2 shows the shaft surging due to turbine/valve closure. Illustration A shows a steady state situation. Illustration B shows the up-surge and C the down surge. This will repeat until the energy is dampened out by friction.

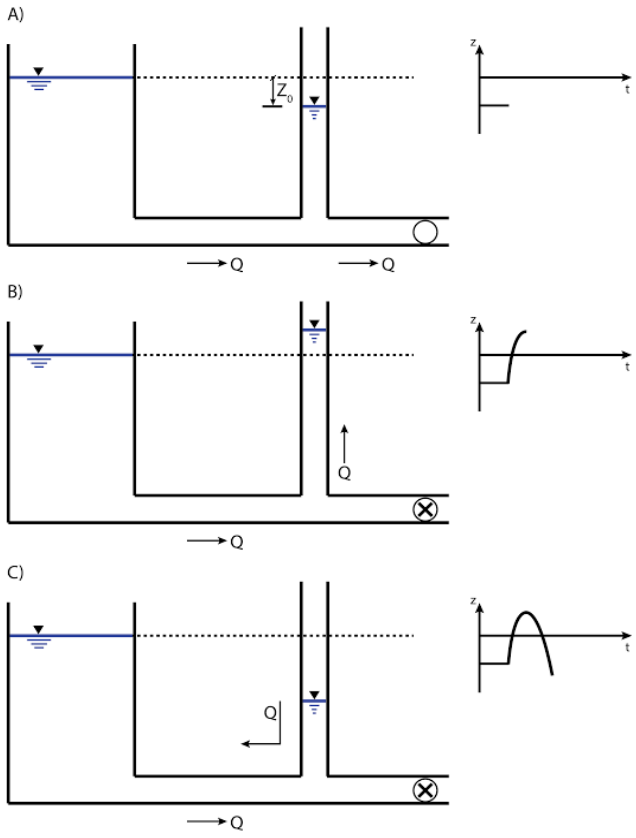

Figure 2: Shaft surging due to turbine closure. Based on Nilsen (1900)

In order to calculate the mass oscillations the continuity (3) and momentum (4) equations, which are referred to in sub chapter 1.2, must be solved. It is first assumed that the elasticity of water and conduit can be neglected. Which means that the wave propagation *a* in the continuity equation (3) can be set to infinite. The continuity equation will then simply reduce to:

$$Q_{in} = Q_{out} \tag{12}$$

Newton second law for a pipe, while neglecting losses and elasticity will be:

$$\rho g(H_1 - H_2)A = \rho LA\frac{dv}{dt} \tag{13}$$

The momentum equation will simplify to an ordinary differential equation by computing the flow as velocity multiplied with area and by adding the head loss term (Nilsen, 1990):

$$H_1 - H_2 - kQ|Q| = \frac{L}{gA}\frac{dQ}{dt} \tag{14}$$

The steady state head loss is proportional to the flow in square. The loss coefficient is given by:

$$k = f\frac{L}{2gA^2D_h} \tag{15}$$

By neglecting losses, the equation of motion for a U-tube and the continuity equation can be combined to express a "thumb of rule" approximation for the surges in shaft (Nilsen, 1990):

$$\Delta z = \pm\Delta Q\sqrt{\frac{L/A_T}{aA_S}} \tag{16}$$

One of the fundamental properties of oscillation is the frequency. The natural frequency of a hydraulic U-tube system can be expressed as angular velocity:

$$\omega = \sqrt{\frac{g}{A_S \frac{L}{A_T}}} \tag{17}$$

The angular velocity is inversely proportional to the time period of the oscillation:

$$T = \frac{2\pi}{\omega} \tag{18}$$

In the literature, the angular velocity is expressed in terms of: Womersley parameter, Strouhal number, Stokes parameter, dimensionless frequency of oscillation and dimensionless frequency parameter. In fact, all of these are somehow related to each other; it is only different ways of expressing the dimensionless frequency.

3.8 Steady State Flow Rate

The time it takes to reach steady state flow from a flow at rest, through a constant diameter and horizontal pipe from a constant head reservoir.

By assuming the friction factor as a constant equal to its steady state value, throughout the transient, it is possible to calculate the time it takes to reach 99% of the steady state velocity. With these assumptions, the governing equation simplifies to (Massoud, 2005):

$$t = \frac{L}{V_0 f\left(\frac{L}{D}\right)} \ln\left[\frac{V_0 + 0{,}99V_0}{V_0 - 0{,}99V_0}\right] \tag{19}$$

3.9 Euler Method – Ordinary Differential Equation

Figure 3 is an example of a simple sketch for a waterway with a reservoir upstream, a surge shaft and a valve downstream.

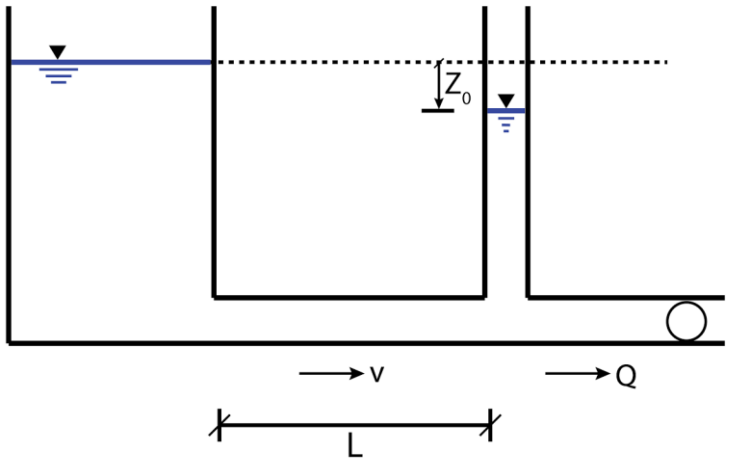

Figure 3: A sketch of a basic system

With the flow Q, and a stationary system the free surface in the surge shaft will be at Z_0 underneath the reservoir level. The difference in height Z_0 is equal to the friction loss in the waterway. If the flow changes, the friction loss will no longer be equal to the height difference Z_0; mass oscillations will occur.

To solve the differential equation, it is convenient to use a numerical solution with systematic integration. A number of finite difference techniques are available to solve the dynamic and continuity equations on a computer. However, studies show that the Euler method gives a sufficient solution for these equations (Chaudhry, 1979).

Euler method is a first order numerical procedure to solve ordinary differential equations where the initial values are known.

Equation 14 computed with respect to changes in velocity:

$$\Delta v = \frac{g}{L}(z - \alpha\, v\,|v|)\Delta t \tag{20}$$

The continuity equation becomes:

$$Q = v\ d + \frac{dz}{dt} A_s \tag{21}$$

Which can be rearrange with respect to changes in surge shaft level:

$$\Delta z = (\frac{Q}{A} - \frac{d}{A} v)\Delta t \tag{22}$$

Equation 20 and 22 are applied to simulate the surge shaft water level for each time step. Minor integration steps are preferable to raise the accuracy.

The initial and following steps are elaborated here:

When t = 0:

- Start with the steady state values. z= z_0, Δv = 0 and $v = v_0$

When t = nΔt:

- Δz_n is estimated by applying equation (22). Use v_{n-1} as input. $z_n = z_{n-1} + \Delta z_n$
- Δv_n is estimated by applying equation (20). Use z_n as input and $v_n = v_{n-1} + \Delta v_n$

3.10 Nyquist Sampling Theorem

In the field of digital signal processing, the required sampling rate for measurements can be calculating using the Nyquist sampling theorem. Sampling is a process of converting a signal into a numerical sequence. The Nyquist sampling theorem gives a prescription for the nominal sampling interval required to avoid aliasing. Aliasing refers to distortion and artefact, i.e. when the signal from the samples are reconstructed differently than the original. Aliasing arises due to insufficiently high sampling frequency.

When the purpose is to reconstruct the original waveform from its samples, the Nyquist sampling theorem says that the sampling frequency should be at least twice the highest frequency contained in the signal (Oppenheim et al, 1989):

$$\frac{\mathrm{fs}}{2} < f \tag{23}$$

4 Measurement Techniques

Measurements are an inevitable method to monitor and control fluid flow, as well as it is an important tool within scientific research. As mentioned, the transition region from laminar to turbulent in a straight pipe is one of the oldest and fundamental problems in fluid mechanics. The knowledge of this complexed phenomenon is limited. However, experiments and transitional models shows that the appearance of stream wise vortices and low-speed streaks plays a crucial role (Brunone et al, 2000). In order to capture these structures, it is a necessity with measurement equipment with high temporal response and spatial resolution.

Temporal response refers to the precision of a measurement in respect to time, while spatial resolution describes the ability to distinguish small details, thereby making it a major determination of image resolution. There is often a trade-off between temporal and spatial resolution.

The main objective of the test rig is to measure the friction loss during mass oscillations. Hence, pressure measurements are essential to find the total pressure loss. If the local wall friction is of interest, it is necessary to measure local velocities. This chapter will review relevant measuring techniques, including basic theory and implementation to research instrumentation.

4.1 Measurement of Pressure

4.1.1 Pressure Transducer

A pressure transducer converts pressure into an analogue electrical signal. Pressure measurements can roughly be divided into three different types: absolute, gage and differential pressure. The absolute pressure measures the difference in pressure at a given point in the fluid flow and the perfect vacuum. Gage pressure measures the difference between the absolute pressure and the local atmospheric pressure. Differential pressure

measures the difference between one unknown pressure with reference to another unknown pressure.

Pressure transducers can be divided into static and dynamic. Static pressure transducers are mostly based on strain gauge, piezoresistive, or capacitive sensing technology. These are capable of measuring slowly changing pressure. Most static pressure transducers have a response limited to approximately 1000 Hz and 1 ms rise time (PCB, 2014). If it is necessary to capture pressure changes that occur faster than this, a dynamic pressure transducer is required. Dynamic pressure transducer most often uses piezoelectric quartz sensing technology; they can respond within microseconds and achieve frequencies well beyond 100 kHz (PCB, 2014).

The highest accuracy of a pressure measurement is attained when the normal operating pressure of the pressure transducer is matched to the application. This includes having a transducer with a pressure range that matches the anticipated pressure, including any spikes or transients (Tavoularis, 2005).

4.1.2 Transducer Connection

There are three configurations for pressure transducers that are commonly applied in the measurement of wall pressure (Tavoularis, 2005): remote connection, cavity mounting and flush mounting. Remote connection through flexible or metallic tubing is the simplest configuration. This approach can be applied to multi-port measurements through the use of manual or automated pressure-scanning valve. This connects a single transducer to a series of pressure taps. An alternative to multi-port measurement is the electronic pressure scanner, which contains a number of small transducers, fabricated by use of semiconductor technology and mounted together on a block, each with a separate pressure port. A disadvantage using remote connection is the deterioration of the dynamic response of the pressure measuring system. This is due to the interference of tubing, connectors and valves. Surface mounting better utilize the transducers capabilities. Surface mounting includes both cavity and flush mounting. Cavity mounting permits the transmission of wall pressure sensed by a small tap, to a nearby transducer and improves the dynamic response compared to the remote connection configuration. However, not either this connection configuration is able to exploit the full capabilities of the transducer. Flush-mounted transducers are the only configuration that are

able to utilize the transducers full dynamic range. This configuration is subjected to two restrictions; the transducers dimensions must be very small and the transducer interface with the flow must match the shape of the surface closely, in order to avoid local pressure distortion. Transducers with flat tips are mainly of piezoelectric and piezoresistive types, they may be mounted only on plane surfaces or when the radius of curvature of the surface is several orders of magnitude larger than the transducer diameter. Small dimensions of the transducers are required to avoid extensive spatial averaging of the measured pressure. This excludes all transducers except for the miniature and MEMS types (Tavoularis, 2005). Differential pressure transducers do not exist with flush mounting.

4.2 Measurement of Flow Rate and Mean Velocity

4.2.1 Ultrasonic Flow Meter

An ultrasonic flow meter uses ultrasound to calculate the flow rate. Ultrasonic transducers emit beams of ultrasound and by averaging the difference in measured transit time between the pulses; the flow meter can measure the mean velocity along a path (Tavoularis, 2005).

4.2.2 Electromagnetic Flow Meter

An electromagnetic flow meter is based on Faraday's law of electromagnetic induction. The flow meter consists of an insulated pipe section of the same diameter as the pipe of interest, surrounded by an alternating or pulsed magnetic field direction. The voltage difference between these electrodes is related to the volume flow rate. They have an accuracy at approximately 0.5 %. However, they are bulky, heavy, and relatively expensive (Tavoularis, 2005).

4.3 Measurement of Local Flow Velocity

Hot-wire Anemometry, Laser Doppler Anemometry and Particle Image Velocimetry are currently the most common used and commercially available diagnostic techniques for the investigation of local velocities in pipe.

4.3.1 Hot-Wire Anemometry

Hot-wire anemometers is one of the most basic measuring techniques; used by researchers and engineers for many years. In spite the new nonintrusive measurement techniques, hot-wire anemometers are still widely applied. Hot-wire is an indirect measuring technique based on convective heat transfer from a heated sensor to the surrounding fluid. The heat transfer relates directly to the fluid velocity. However, a simple hot-wire will not have the sufficient response time for measuring flow fluctuation. Hence, the development of the constant temperature system. Figure 4: CTA set up (Dantec Dynamics, 2013) Shows the configuration of a traditional CTA system.

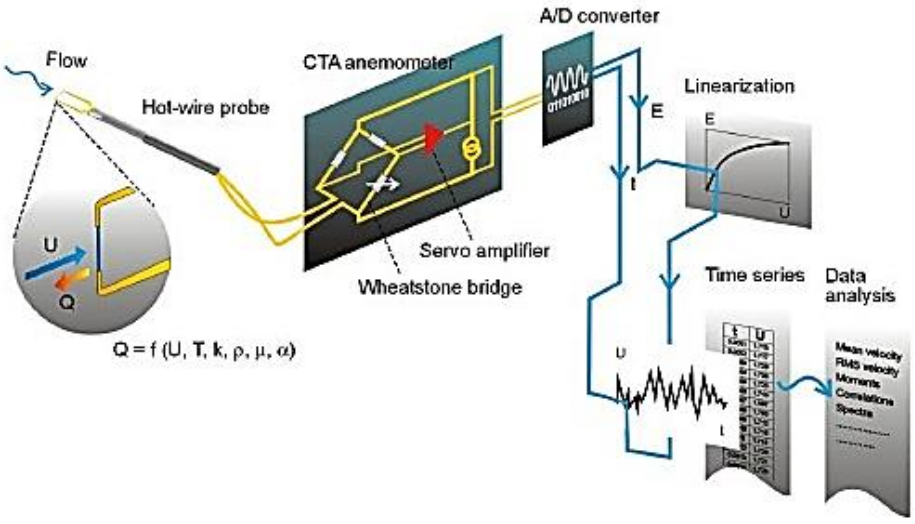

Figure 4: CTA set up (Dantec Dynamics, 2013)

By adding a feedback loop to the traditional hot-wire converts the anemometer to a constant temperature system, (CTA). In a CTA, the velocity is measured by its cooling effect on a heated sensor. The sensor temperature is kept constant by a feedback loop in the electronics. Heat is generated when fluid passes the wire. The system has equilibrium when the heat generated is balanced by the heat loss to the surroundings. If the velocity changes it causes the

convective heat transfer coefficient to change. Resulting in a wire temperature change that will eventually reach a new equilibrium with the surroundings. The voltage drop across the sensor becomes a direct measure of the power dissipated by the sensor. A CTA is adequate to follow flow fluctuations up to several hundred kHz. Dimensions of the wires are normally; 5 mm in diameter and 1.2 mm long suspended between two needle-shaped prongs.

The probes are available in one-, two- and three-dimensional versions. The sensors respond both to magnitude and direction of the velocity vector, information of both can be obtained when two or more sensors are placed under different angles to the flow vector (Jensen, 2004). The most common measurement is the use of a single hot wire, perpendicular to the flow, to measure mean velocity and fluctuations in the mean flow direction. By using a cross-wire or X probe it allows for measurement of two components. An X-probe consists of two wires arranged in an X configuration. Three components can be measured by adding a third sensor. However, the maximum turbulence intensity that can be measured is still limited. For instance, changes of flow directions cannot be detected.

For measurements in liquids, especially water, film sensors are more suitable than wire sensors. Film sensors permits flexibility in shape, which can give advantages in terms of strength and the ability to remain clean in contaminated fluid. Hot film sensors made for water have a heavier coating of quartz, which provides complete electrical insulation (Goldstein, 1996, s152).

Table 1 present the relevant probes for use in water, based on Dantec´s probe selection guide (2015):

Table 1: Probe selection chart.

X = Recommended **Y = Applicable** **• = Not applicable**	**Fiber-film probes (One sensor)**	**Flush mounting probes (One sensor)**	**Fiber-film X-probes (Two sensors)**	**Fiber-film triple sensor probes (Three sensors)**
Water as medium	X	X	X	Y
Little space	•	X	•	•
Mean velocity	X	•	X	X
Instantaneous flow direction	•	•	X	X
Velocity fluctuations	X	X	X	X
Low and medium turbulence intensities	X	•	X	X
High turbulence intensities	X	•	X	•
Turbulent shear stress	Y	•	X	X
Wall shear stress	•	X	•	•

The probes are mounted in a hole in the pipe wall. Flush-mounting probes are mounted orientated perpendicular to the flow. X-probes are mounted with the probe axis parallel to the direction of the main flow. Therefore, the dominant flow vector attacks the two films at 45 °. Triple-sensor probes are mounted with the probe axis in the main flow direction (Dantec, 2015).

Some limitations have to be taken into account when it comes to intrusive probes. Firstly, intrusive probes are subject to non-linearity and requires calibration. Secondly, it is sensitive to variables in the fluid flow. Thirdly, it interferes with the physical process and it is therefore exposed to breakage.

The system configuration for CTA is the process of mounting and interconnect the selected probes, cables, CTA anemometers, signal conditioner and A/D channels. Standard probe cable length is 4 metres plus 1-metre support cable (Dantec, 2002).

4.3.2 Laser Doppler Anemometry

LDA is a non-intrusive measurement technique that measures the velocity of particles. The LDA utilizes the Doppler Effect to measure instantaneous particle velocities. The Doppler Effect is normally associated with the moving source of sound, for instance a siren. The faster moving source of sound, the greater the shift in frequency. This principle is also valid for light, and is the basic working principle of a LDA. The particles (typically, 0.1 – 10 μm) in the flow are illuminated with a laser beam, the frequency of the light scattered from the particles is different from that of the incident beam. This frequency is linearly proportional to the particle velocity, and is called the Doppler shift (Jensen, 2004).

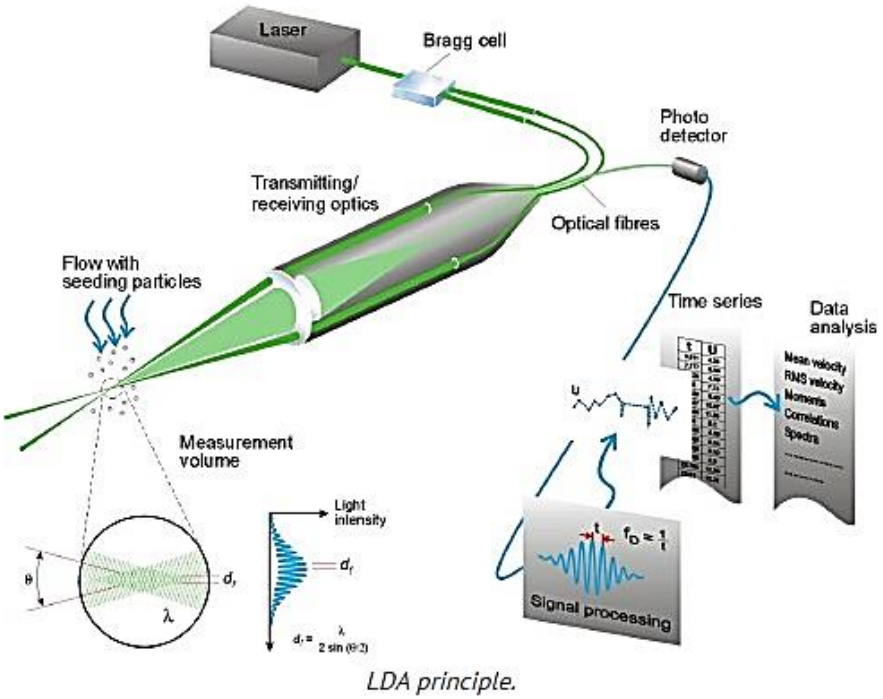

Figure 5: A backscatter LDA system for one-velocity component measurements (Dantec Dynamics, 2013).

The basic configuration consists of a continuous wave laser, transmitting optics, receiving optics, a signal conditioner and a signal processor. Transmitting optics includes a beam splitter and a focusing lens. A beam splitter sends out incident laser beams of different wavelength, the output of this cell is two beams of equal intensity with frequency f_0 and f_{shift}. A bragg cell is often used as a beam splitter. The beams are brought to a probe where they are focused by a lens to intersect in the measurement volume, which creates a fringe pattern in the measurement volume. The fringe pattern consists of alternating zones of brightness and darkness. The fringe spacing is the distance between the alternating zones. When the particle crosses the fringe pattern, the intensity of the scattered light varies with the intensity of the fringes (Albrecht et al. 2002).

The measuring volume is an ellipsoid and takes place in the intersection between the two incidents focused laser beams. The thickness, i.e. the diameter of the measurement volume is given by the beam thickness at the beam waist. The thickness of the measurement volume is proportional to the laser beam thickness (Zhang, 2010). Typical dimensions for measurement volume are in order of 0.05 – 0.1 mm thickness and a finite length of about 0.5-3 mm, again depending on the optical arrangement of the laser (Zhang, 2010). Smaller measurement

volumes can be achieved, however, fewer fringes in the measurement volume increases the uncertainty of Doppler frequency estimation. The temporal resolution depends on the concentration of seeding rather than the measuring equipment itself (Dantec Dynamics, 2013). It is recommended to use seeding particles that are larger than the wavelength of the laser light and small enough to be good flow trackers. The necessary laser power depends on many factors, including flow velocity, scattering efficiency of the particles, position and focal length of the receiving optics and the flow medium.

Because it is a linear relation between the Doppler frequency and the velocity, the LDA requires no physical calibration prior to use. Commercial LDA signal processors can deal with data rates in the ten kHz range to hundreds of kHz range (Jensen, 2004)

LDA set up can be in either back-scatter mode or forward-scatter mode. Meaning that the receiving optics are positioned opposite or at same side of the transmitting aperture. Backward scattering LDA allows for the integration of transmitting and receiving optics in a common housing, which saves the user time-consuming work aligning separate units. However, forward scattering is beneficial in some flow studies. For instance, the investigation of transient phenomena, as this requires high data-rates in order to collect a reasonable amount of data over a very short time.

Combinations of Laser Doppler systems with component separation based on colour, polarization or frequency shift allows one-, two- or three-component LDA systems to be put together based on common optical modules (Albrecht et al. 2002). A one-velocity component system is mostly designed to be rotated about the optical axis, which allows for consecutive measurement of different velocity components at the same position in the flow field. For instance, a dual beam configuration can be made by creating a support platform for the LDA head and mount it on a traversing board. The dual measurement method is conducted simply by rotating the LDA head around 180 degrees. Through twice measurements of the same flow the velocity shift as the outcome of the LDA alignment error can be identified. Which leads to direct determination of the tangential velocity component (Zhang, 2010). However, this is only adequate for stationary flow.

Extending a one-velocity component laser to two velocity components requires a second measurement volume with a different orientation about the z-axis. The most common set up is a two colour, four-beam arrangement. However, simultaneously two-component velocity measurement, by using two pairs of laser beams, cannot be carried out in circular pipe flow,

as the four beams do not intersect at a unique point in the flow because of the optical aberrations (Zhang, 2010).

Measurements of all three-velocity components in pipe flow could only be achieved one after another. A great number of LDA measurements in pipe flow have been restricted to axial and tangential velocity components. The measurement of tangential velocity component does not represent a highly difficult task. In contrast, the measurement of radial velocity component is a very complicated task. There are almost no such measurements that have been carried out or can be referred to (Zhang, 2010).

Direct pipe flow measurements result in optical aberration in the receiving optics, which results in disturbances in the measurements. Experiences show that in traversing the velocity profile across a circular pipe, the signal rate can only be achieved within a depth of about 1/3 of the pipe diameter. To measure the flow in the centre area of a circular pipe it is necessary to match the refractive index of the flow to that of the pipe wall (Zhang, 2010).

Putting the circular pipe into a rectangular water tank with plane walls, are one of the commonly applied methods to reduce the optical aberration. Such a measurement facility will enhance the optical performance. However, the problem of calculating the measurement volume remains because each laser beam still suffers from two-time refraction on the curved interfaces. Another method to improve the optical performance can be obtained by cutting of the outside of the pipe and make it plane. The main optical aberration is then only restricted to the beam refraction on the internal surface of the circular pipe. This approach allows to obtain high quality signals even at a distance of 2/3 of pipe diameter from the pipe wall (Zhang, 2010).

4.3.3 Particle Image Velocimetry

Particle Image Velocimetry (PIV) is a non-intrusive measurement technique, which makes it possible to capturing velocity information from the whole flow field in a fraction of a second. Figure 6 shows an example of the experimental set up (Raffel et al., 2006).

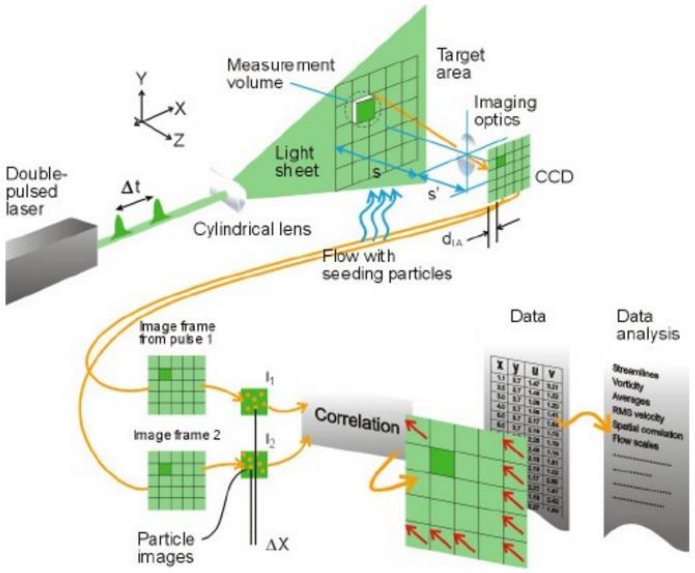

Figure 6: PIV set up (Dantec Dynamics, 2013)

The technique is based on images of tracer "seedings" particles suspended in the flow. By measuring local fluid velocity by measuring the fluid displacement from multiple particle images and dividing that displacement by the time interval between the exposures. The PIV measurements works by illuminating a cross section of the seeded flow field, recording multiple images of the seeding particles using a camera located perpendicular to the light sheet, and analysing the images for displacement information. The reordered images are divided into interrogation areas; the dimensions of which determine the spatial resolution.

There are several methods for image processing. One of them is based on capturing multiple images on a single frame, and then the displacement can be calculated by auto-correlation analysis. However, the common method is to capture two images on two separate frames, and perform cross-correlation analysis.

By increasing the time difference between the images the accuracy and dynamic range increases. However, it also decreases the likelihood of having common particles in the

interrogation area. A known rule of thumb is to insure that within the time difference the velocity component V_x and V_y carries the particles no more than a third of the interrogation area dimensions (Raffel et al., 2006).

Typical interrogation regions for PIV are 32 x 32 pixels. This would correspond to a sensor having dimensions of 3 mm x 3 mm and a light sheet thickness of 1 mm. When taking an image of area 10 cm x 10 cm using a digital camera with pixel format 1000 x 1000 pixels (Raffel et al., 2006).

The PIV technique also has a linear calibration response between the particle displacement and the particle velocity. PIV calibration involves measuring the magnification factor for the image. This is carried out by placing a calibration plate in the flow field.

Using laser as a source of bright illumination is not a requirement, but is often chosen over white light sources. This depends on the illumination requirement for the specific measurement. The size of the tracer particles is often a compromise between having small particles in order to follow the flow faithfully and the need to utilize larger particles because of their better light scattering efficiency.

The traditional PIV method is only capable of recording the projection of the velocity vector; the out-of-plane velocity component is not recorded. The most common technique to measure all three-velocity components is called “Stereoscopic PIV” (SPIV), and involves using an additional camera, viewing the flow from two different angles. Each camera measures the particle displacement perpendicular to its viewing direction. Two different projections of the velocity are obtained. From these projections, the out-of-plane velocity vector can be reconstructed. In SPIV measurement, the light sheet thickness becomes an important parameter that determines the balance between the spatial resolution and signal to noise ratio. Measurements in a circular pipe and 3-D stereoscopic PIV, requires calibration and documentation of the perspective distortion of target images obtained. In practice, it is a complicated process to obtain the three velocity vectors. The literature reports three main approaches.

The approach presented here is suited for rather fast processing time: first 2C displacement for each view are computed on a regular grid, evaluated by standard PIV method. Then the 2C-vector fields must be mapped from the images planes and onto the measurement plane of the light sheet. Finally, they have to be interpolated on a common grid. This combines the

displacement vectors from both cameras, and makes it possible to reconstruct the three components of the particle displacement (Raffel et al., 2007, s.215). The errors related to these steps are important to consider when evaluating the accuracy of the measurements.

The advantage using PIV is the possibility to quantify the whole flow field. However, the PIV sensors can have limited temporal resolution due to the framing rate of the cameras and the pulsing frequency of the light source. Most common video cameras used today operates with 30 Hz, with lasers pulsing at 15 Hz. Hence, the system samples velocity fields at 15 Hz. Modern developments of camera and laser technology continues to improve. For instance, CCD cameras, CMOS/based digital cameras and copper vapour lasers permits PIV measurements in the ten kHz framing rate. However, the computational resources needed in processing the image information still limits its common use.

When investigating internal flow with optical measuring techniques it is important to consider the optic aberration, as discussed in the previous sub-chapter. When fluid is viewed through curved walls, the optic view is distorted. These distortions reduce to some extent when using pipe walls as thin as possible. One solution to further reduce the refraction is to implement a liquid filled prism to compensate for astigmatism (Albrecht at al. 2002). Another solution is to do refractive index matching, which refers to the technique of matching the refractive index of the flow liquid to that of the transparent window. The methods presented for LDA are also valid for PIV measurements.

4.3.4 Strengths, Limitations, and Comparison between CTA, LDA and PIV

Based on some important criteria of measuring techniques CTA, LDA and PIV are compared. Table 2 is based on studies from K. D. Jensen (2004).

Table 2: Comparison of commonly used velocity measurement diagnostics.

	CTA	**LDA**	**PIV**
Frequency response	Very high: Hundreds kHz range	Good: Typically ten kHz, may reach hundred kHz range	Particle motion frozen at 2 instants in time. Depends on the framing rate. Common 15 Hz. Possible to reach ten kHz
Spatial resolution	Typically; 5 µm diameter x 1 mm	Thickness of the measurement volume is about 0.005-1 mm and a finite length of 0.5 – 3 mm	Depends on the chosen measurement volume. Typically, 32 x 32 pixels, which corresponds to a sensor; 3 mm x 3 mm
Resolution	Typically, 12- and 16- bit; can be higher	16 bit digitization of Doppler frequency within selected bandwidth	Typical 6- to 8- bit- Depends on subpixel resolution of particle displacement
Physical interference	Yes	No	No
Influence of other variables	Yes	No	No
Proportionality of output signal	Non Linear	Linear	Linear

- Calibration:

A CTA sensor is affected by flow variables and needs to be calibrated for their velocity response, as well as for their angular response. For multi wire probes, it is necessary to calibrate the cosine angular response of the wires to the cooling velocity (Jensen, 2004).

LDA requires no physical calibration. The measurements are based on the relation between velocity in the plane of the laser beams, distance between the fringes and the Doppler frequency. As the distance between the fringes is a constant for a given optical system, there is a linear relation between the Doppler frequency and velocity.

PIV calibration is done by measuring the magnification factor for the images as well as documenting the perspective distortion. To magnification factor is measured by implementing a calibration plate in the measurement volume.

For LDA and PIV measurements, it may be necessary to filter the water to remove natural foreign particles, such as dust, lint and microorganisms. Before the water is seeded with particles whose characteristics are suitable for the purpose of the study.

5 The Water Power Laboratory

The Water Power Laboratory was built in 1917. Figure 7 shows a 3D drawing of the building and the main system. Today there are various pipe-loops, pressurized through centrifugal pumps. The laboratory has a unique upper free surface reservoir, in addition to closed loop test circuits (NTNU, 2015). The amount of existing test rigs in the laboratory limits the space available.

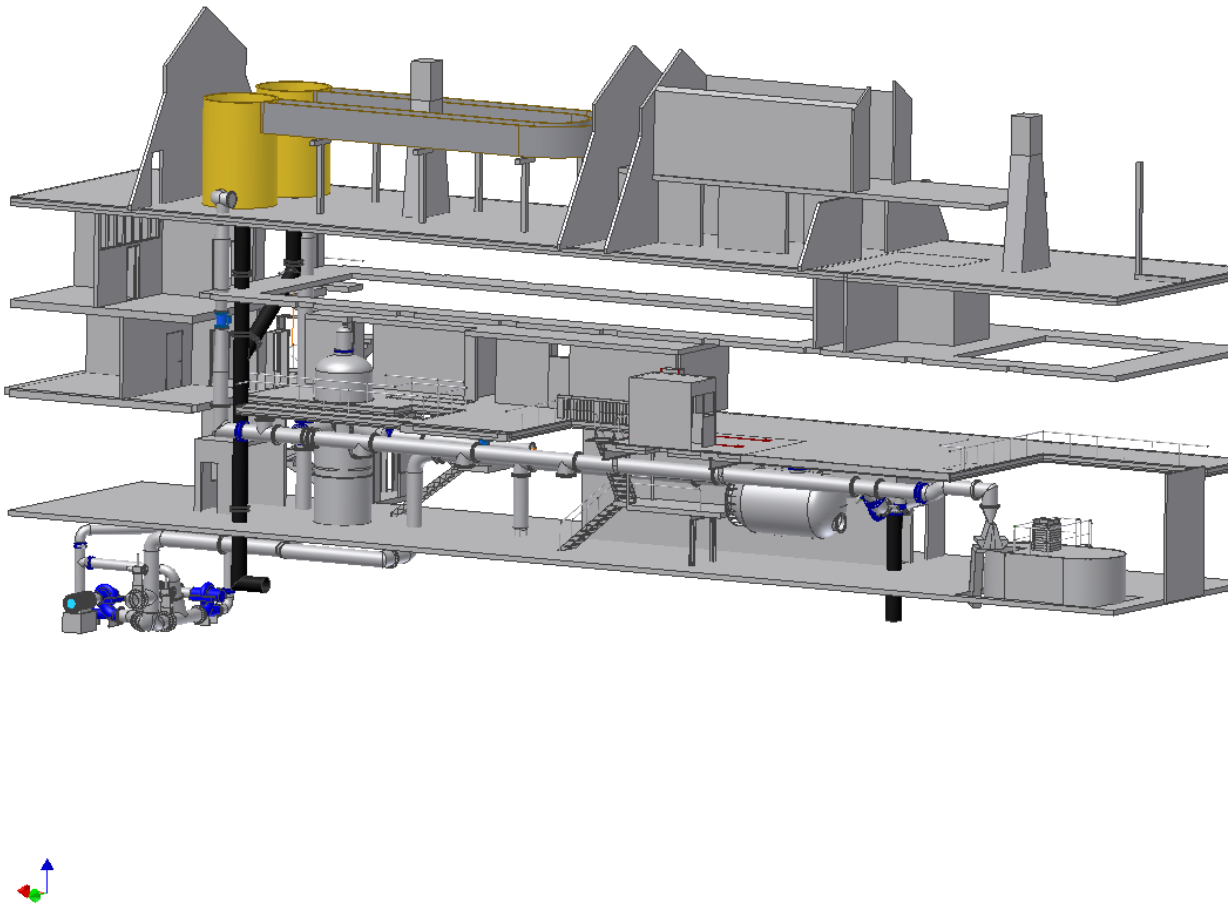

Figure 7: The main system in The Water Power Laboratory

5.1 Laboratory Constraints and Existing Infrastructure

The first floor (above the ground floor) is the designated area for construction of this test rig. The laboratory has limited space available, which makes it important to evaluate the existing infrastructure and constraints.

- There is a traverse crane mounted three meters above the floor of the first floor in the laboratory. The traverse crane limits the accessible height from the floor to three meters
- The floor is constructed with steel beams. Some areas have wooden decking, and others have steel plates or steel grids. Depending on the weight of the test rig, the location may be restricted to certain areas that have the required floor strength
- The second floor is not coherent; it has several large openings down to the ground floor. Shown in Figure 7 and Figure 8
- The main water discharge, the sump, is located in the basement of the laboratory
- There are regular water hosts available, they have a flow rate of 1 l/s
- The main system in the laboratory has two centrifugal pumps, each with 330 kW and a capacity of 800 l/s. These pumps provide the main system, as well as external test rigs, with the necessary flow rates
- The Pelton loop is connected to an external centrifugal pump, which provides the turbine with water from the sump. The Pelton turbine is located on the first floor, while the pump is located on the ground floor. This centrifugal pump is not used by the main system. The pump has a power of 1.75 kW
- The laboratory is equipped with a compressed-air system that provides service air and instrument air at 6 bar. There is also a small hydraulic unit. Both available for use as an operational energy source for a possible actuator

Figure 8 shows the first floor of the laboratory.

Figure 8: Picture of the first floor. Picture taken from northwest.

5.2 Available Measurement Equipment

The Water Power Laboratory is a research laboratory and has various measurement equipment available. There are a number of different pressure transducers, including four PTX static pressure transducers ranging from 0-2.5 bar absolute. There are digital to analogue converters that can operate with either 4-20 mA or 2-10 V output from the pressure transducers.

5.3 Purchased Components

The establishment of such a test rig has been a desire for several years at The Water Power Laboratory. The following components have already been purchased for this project:

- An ultrasonic flow meter. Purchased from KROHNE instruments, DN150
- 4 x 6 metres stainless steel pipes. The pipes have an inner diameter of 150 mm
- A tank with a volume of 2500 litres. The tank was originally constructed to contain milk and has a layer of foam insulation between the outer and an inner layer. The tank still has its original components. Figure 9 shows the dimensions of the tank:

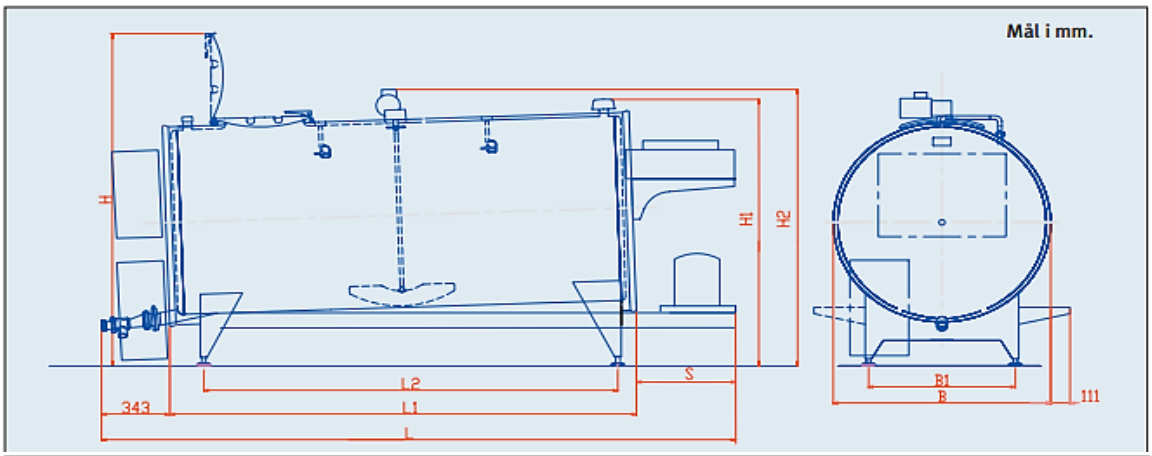

TYPE	VOLUM LTR	B	B 1	H	H 1	H2	L	L1	L2	S	VEKT KG
25AL	2500	1250	840	2020	1650	1720	3620	2775	2325	520	580

Figure 9: Tank dimensions (Landteknikk, 2005)

6 Test Rig Set Up

The centrepiece of the test rig is the test section, where measurements are conducted. All devices and components of the apparatus, which are not directly linked to the measurements, serves the purpose of producing the desired flow through the test section.

The design of the test rig is based on the waterway in a hydropower plant. The basis of the layout consists of an upper reservoir, a waterway, a surge shaft and a valve downstream the surge shaft. Water is the working fluid.

The following chapter goes through the devices and components that are necessary to produce the desired flow through the test section.

6.1 Upper Reservoir

The flow is lead through the test section by a constant head in the upper reservoir, which requires water supply, spillway and discharge. The use of this method, to keep a constant pressure level, can cause unwanted circulations in the reservoir. The circulations can be kept to a minimum with a reservoir that has a large volume, relative to the the flow rate. However, a large volume means increased weight, which makes it important to consider the floor strength required.

6.1.1 Spillway

Spillways are structures that control the water level in a reservoir. A spillway is essential to avoid a higher water column during the returning oscillations and in case of unnecessary water supply. The spillway need a sufficient capacity to lead the water away. Depending on the reservoir characteristics, there are several methods to implement a spillway, but can roughly be described as:

1. External spillway: external spillways have the interface in the wall of the reservoir, immediately leading the water out of the reservoir. The capacity of an over fall spillway can be expressed as (Guttormsen, 2013):

$$Q = C_d L H^{1.5} \tag{24}$$

The discharge coefficient depends on the depth from the crest to the bottom of the reservoir, slope upstream face and influence from the downstream water.

2. Internal spillway: internal spillways are located inside the reservoir, connected to a pipe that leads the water away. Spillways constructed inside dam reservoirs are often referred to as morning glory spillways. The discharge in morning glory spillways is expressed as (Bagheri, A., et al, 2010):

$$Q = C_d L H^{1.5} \tag{25}$$

$$L = 2\pi R_s \tag{26}$$

Researchers have not yet found a solution for the discharge coefficient for morning glory spillways. However, Bagheri et al. (2010) developed an empirical equation using experimental data:

$$C_d = 2.967\left(\frac{H}{R_s}\right)^{0.178} \tag{27}$$

Determination of a spillway structure is dependent of the geometry and material of the upper reservoir and has to be evaluated closely with the reservoir characteristics.

It is desirable to both have a spillway that results in a reservoir head of 1 MWC and 2 MWC.

6.1.2 Discharge

The test rig will discharge water both through the spillway in the upper reservoir and downstream the surge shaft. This water can either be lead down to the main discharge in the

basement of the laboratory, or it can flow in an internal loop. The discharge in the laboratory basement is easily accessible.

6.1.3 Supply Water Inlet

The interface between the supply pipe and the upper reservoir must be considered carefully. The location and design must be chosen to ensure minimal impact on the existing water in the tank. If the water inlet is located above the water surface, it will be necessary to implement an energy dissipater to avoid additional pressure variations. The dissipation of energy in fluid flow is created through internal friction and turbulence, or impact and diffusion of the high velocity flow.

6.2 Surge Shaft

A surge shaft will be placed along the waterway. There are various ways to create a surge shaft; however, the focus will be to design a shaft that induces minimum losses to the flow. It is also a desire to have a flexible surge shaft, which can be rearrange to change the length of the waterway.

6.3 Waterway

The waterway is the distance between the upper reservoir and the surge shaft. The stainless steel pipes that will form the waterway are already purchased. The waterway will be constructed in a straight horizontal line. It is desirable to construct the longest waterway possible in the laboratory, with the opportunity to rearrange it.

6.4 Minor Losses

An ideal test rig will not be influenced by any other factors than the friction to be measured. Unfortunately, this is not possible in practice as there always will be minor losses. However, the minor losses can be kept to a minimum. A brief presentation of relevant areas that induces minor losses follows (Rennels, Hudson, 2012):

- Pipe entrance: the pressure loss at the pipe entrance is affected by the distance from the pipe edge to the wall, the thickness of the inlet pipe edge, the angle at which the pipe is mounted into the wall and the degree of rounding or bevelling of the edge of the pipe inlet. For the case of generously rounded entrance the loss coefficient becomes (Rennels, Hudson, 2012):

$$K = 0.03 \quad \left(\frac{r}{d} \geq 1\right) \tag{28}$$

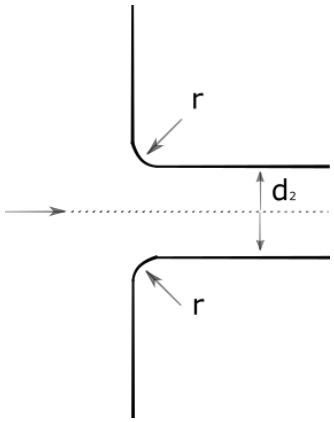

Figure 10: Pipe entrance

- Contraction: a sudden contraction will cause the flow to accelerate as it approaches, resulting in high radial velocity that creates a flow separation. The high radially inward velocities can be reduced by rounding, tapering or bevelling the entrance to the contraction. This reduces the head loss significantly. The main geometric considerations are the diameter ratio, $\beta=d_2/d_1$ and the length of the conical section. Relation of the loss coefficients and geometry are found in Figure 10.3 in Rennels & Hudson (2012).

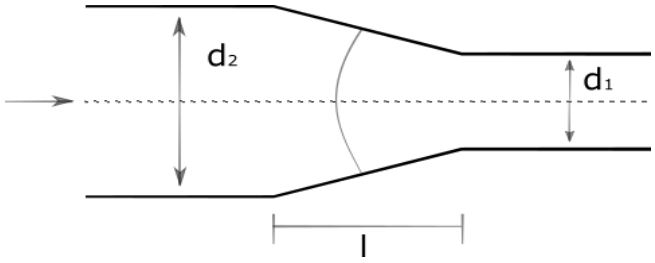

Figure 11: Gradual connection

- Tee junction: the energy loss at a pipe junction depends on the direction of the flow, the proportion of the flow division and the geometric properties. The geometric properties are the angle of the branch, branch to junction diameter ratio, and curvature of the joining edge. The pressure loss in a tee junction can be reduced by rounding of the branch edge. Rennels and Hudson (2012) indicates that a radius ratio, $r/d_{branch,}$ of 0.10 is reasonable, which corresponds to 50 % of the benefit of rounding. By enhancing the radius ratio to 0.3, 90 % of the benefit of rounding the edges can be reached.

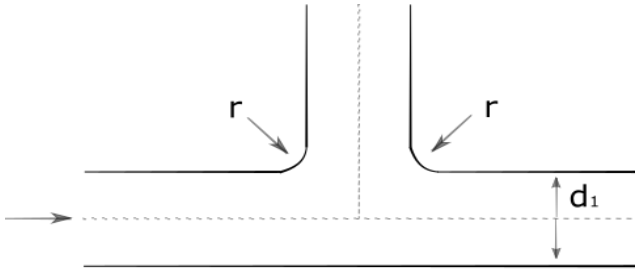

Figure 12: Tee junction

- Pipe joints: Pressure loss due to pipe connections or joints can sometimes contribute to significant pressure loss. Especially if threaded pipe connections are used. They offer a greater pressure loss due to the internal geometry. Flanged or socket weld connections serves minimal pressure losses, unless they are terribly misaligned.

6.5 Supply Water

There is a number of different alternatives to lead a sufficient water supply to the test rig.

1. Connect the test rig to an existing pipe-loop system.
    - Pelton loop:
        - Maximum flow rate of Q= 25 l/s
        - Connected to a centrifugal pump at the ground floor
        - The pump works independent of the main system
        - Requires small modifications to connect these systems
    - Pressure-time loop:
        - Maximum flow rate of Q= 400 l/s
        - Connected to the two main centrifugal pumps in the laboratory
        - Limited availability, as these pumps are frequently used
        - Requires small modifications to connect these systems
    - Free surface reservoir:
        - Can reach very large flow rates
        - Provides a large head
        - Requires relatively large modifications to connect these systems
        - Uses the two main pumps to fill up the reservoir
        - The free surface reservoir is in use when the main system runs in open loop; this is not as frequently in use as the closed loop system
2. Internal loop: An alternative is to construct an internal loop
    - Water host: there are a few water hosts available in the laboratory
    - Pump system: Purchase a pump to create an internal system for this test rig, independent from the rest of the laboratory

6.6 Flow Management

Valves, actuators and sensors are necessary to control and manage the flow in the system and are a necessity when it comes to safety.

To initiate the mass oscillation, it is necessary with an immediately shut- off valve downstream the surge shaft. This valve will also work as the control valve that regulates the flow rate through the test rig.

The system contains a relatively large amount of water. It is therefore necessary to have the possibility to shut down parts of the system to have full control, in case of leakage or other undesired situations.

6.6.1 Valves and actuators

There are various types of valves, where each serve a specific purpose. They all have their advantages and disadvantages. It is therefore important to choose the optimum one for its application. Valve selection should always be based on function, design extremities, end connections, operation, weight, availability, maintenance and cost.

Regarding design extremities, it is important to consider the possibility of cavitation. This is especially a challenge for control valves. Cavitation can occur if the speed through the valve increases so much that the pressure in the fluid drops to a critical value, which corresponds to the vapour pressure of the fluid. This will cause the fluid to boil, creating bubbles filled with steam. The implosion of the bobbles causes cavitation, leading to mechanical vibrations, noise and material erosion (Samson, 2003).

A brief presentation of the advantages and disadvantages of relevant valves follows (Smith, 2004):

Valves:

- Gate valve: minimal pressure loss through the valve. Bidirectional. Cannot be quickly opened or closed, not suitable for regulate or throttle flow
- Globe valve: primary designed to stop, start and regulate flow. Can be used where pressure drop through the valve is not a controlling factor
- Ball valve: Quick on/off application, with low-pressure drop. They are sometimes used for flow control. Tight sealing with low torque. Minimum resistance
- Butterfly valve: generally used in low pressure, large diameter lines. Very low-pressure drop and lightweight. Easy to open/close, but limiting throttling services
- Check valve: are automatic valves that opens with forward flow and closes with reverse flow. These valves are particularly important in the case of pumps and compressors, where back flow can cause damage
- Needle valve: applied in situations where the flow is gradually brought to a halt, and where precise adjustments of flow is necessary, or where a small flow rate is desired. The design resembles that of the globe valve. Needle valves is a volume-control valve that allows for precise regulation and are easy to shut off completely

Valve actuators serves the purpose of moving or controlling the valve. An actuator may be required due to control, inaccessibility, emergency shutdown/fail-safe, excessive valve operating torque or/and safety. The actuators can have different working principle and can operate with different source of energy. A brief overview of actuators with different source of energy follows (Smith, 2004):

Actuators:

- (Manual actuators: hand wheel attached to the stem directly)
- Pneumatic actuators: uses compressed air to provide the force to position the valve. This is the most common type of actuator, because they are cheap and readily available power source. Less complex, and easy to maintain
- Electric actuators: connected to the stem through a gear train that reduces rotational speed and increases torque. Smooth operation, stability and high torque values. However, they are expensive, complex and must be protected from moisture
- Hydraulic actuators: uses a pressurized liquid to provide the force required to position the valve. These actuators are capable of delivering very high torques, and can operate larger valves. Often are hydraulic actuators used when pneumatic or electric motors are either not suitable or not available

6.6.2 Water level sensors

Level sensors and switches are necessary to control a reservoir. Several methods to measure fluid level in a reservoir are summarized below (Sensormag, 2016):

- Load cells: A load cell is a mechanical support bracket equipped with sensors that detect small distortions in the support member. The load cell must be a part of the vessel's support structure. When a force on the load cell changes it causes the brackets to flex, which results in changes in the output signals from the sensors. Load cells are advantageous in many applications because they are non-intrusive. However, load cells are expensive and the design of the support structure must be coincident with the load cell requirements

- Pressure transducer: the pressure at the bottom of the reservoir equals the water column. Detailed information about pressure transducers can be found in chapter 4.1.1.

- Ultrasonic level transmitter: measures the distance between the transmitter and the surface, by using the time required an ultrasound pulse to travel from a transmitter to the fluid surface and back

- Laser level transmitter: Operates similar to ultrasonic level transmitter. Instead of using the speed of sound, it uses the speed of light

- Float level transmitter: uses the simple principle of buoyancy, by placing a buoyant object on the water surface and connecting it to a mechanical device

6.7 Test Section

The test section must be located where it can ensure fully developed velocity profiles. The design of the test section depends on the measurement techniques applied. The dimensions, material and space around the test section are important criteria to consider.

7 Results and discussion

The results are going to be presented and discussed. The underlying arguments behind the results were a combination of: the desire to produce the specific flow through the test section, laboratory constraints, flexibility and the existing components. The focus has been to clarify possibilities and constraints, in contrast to suggesting one specific solution.

Firstly, the possible flow situations are identified and simulated. Secondly, the recommended set up of the test rig is presented. Thirdly, the test section design is specified for the respective measurement techniques. Finally, a table summarizes the recommended measurement technique for each specific field of interest.

7.1 Calculated Input Parameters from the Flow

This sub chapter presents the flow situations that are possible to obtain in the laboratory. The calculations were prepared to support the establishment of flow rates and system pressure.

7.1.1 Possible Dynamic Flow Situations

Six possible flow situations were simulated. The flow situations were based on different test rig layout, and the desire to obtain the largest flow rate possible. However, this was limited by the constraints in the laboratory. The simulations were carried out with Euler’s integration method.

The constant parameters (Table 3) are known due to either; laboratory constraints, existing materials, water properties or assumptions taken.

Table 3: Constant parameters

Parameter	**Dimension**	**Unit**	
Kinematic viscosity	1.31E-06	m^2/s	v/10°C
Density	999.71	kg/m^3	v/10 °C
Gravitation	9.81	m/s^2	
Roughness stainless steel pipe, ε	0.002	mm	
ε/D	1.33E-05	-	
Waterway			
Diameter	0.15	m	
Cross section area	0.018	m^2	
Surge shaft			
Diameter	0.15	m	
Cross section area	0.018	m^2	
Height	2.50	m	

The variables in the test rig layout were pressure level and length of the waterway. The pressure level in the upper reservoir was set to either 1- or 2- metres water column. The length of the waterway was set to either 11-, 18- or 29-metres.

The different test rig layouts resulted in different flow rates. The variable parameters for each flow situation are presented in Table 4.

Table 4: Variable parameters

Flow situation:	**1**	**2**	**3**	**4**	**5**	**6**
Design flow rate [m^3/s]	0.005	0.011	0.013	0.006	0.016	0.008
Velocity [m/s]	0.28	0.62	0.74	0.34	0.90	0.42
Reynolds number	3.24E+04	7.13E+04	8.42E+04	3.89E+04	1.04E+05	4.86E+04
f - friction coefficient	0.023	0.019	0.019	0.022	0.018	0.021
Head loss [m]	1.82E-02	7.41E-02	6.19E-02	1.57E-02	5.49E-02	1.42E-02
k - loss coefficient	0.23	0.20	0.11	0.14	0.07	0.08
Length [m]	29	29	18	18	11	11
Pressure height [m]	2	1	1	2	1	2
Time period [s]	11.3	11.3	9.1	9.1	7.4	7.4
Frequency [Hz] [1/s]	0.56	0.56	0.69	0.69	0.85	0.85

The friction factors were determined by assuming fully turbulent flow and calculated by iterating Colebrook's equation, which depends on the Reynolds number and the relative roughness. The friction factor varies during the oscillations and will most likely alternate between laminar and turbulent regimes.

The exact roughness of the stainless steel pipes is difficult to specify; it was therefore assumed equal to the overall assumed roughness of stainless steel pipes.

The transition from laminar to turbulent in pipe flow has the general accepted value of the Re = 2300, which is known as the critical Reynolds number for pipe flow. However, the critical Reynolds number is different for different geometries and flow conditions. Which means that, even though all six simulated flow situation have an initial Reynolds number higher than 2300, it is still not certain that turbulent flow is triggered. However, the estimates show initial Reynolds numbers at 10^4 regions, in which it is naturally to assume the occurrence of turbulent flow.

Figure 13 shows a simulation of the oscillations in the surge shaft for flow situation 1 and 5:

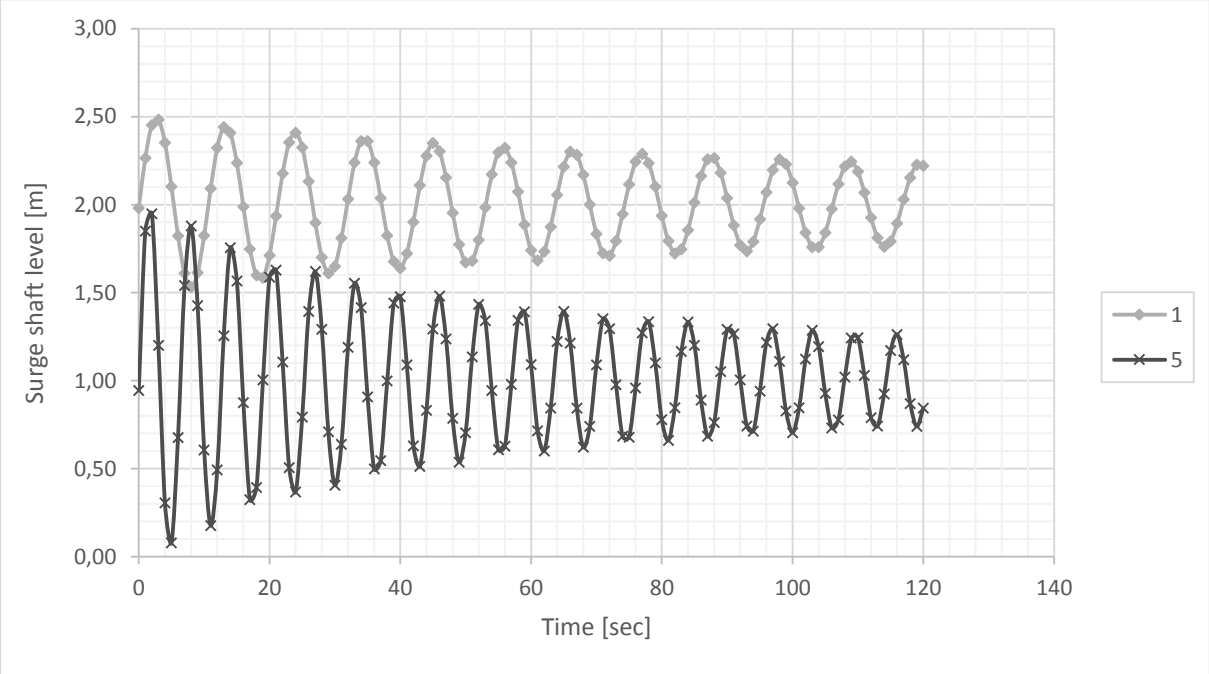

Figure 13: Simulated oscillations in the surge shaft

Observing the simulations, it can be seen that the design flow rate for 1 MWC was limited by the maximum down-surge. In contrast, the design flow rate for 2 MWC was limited by the maximum up-surge.

A longer waterway increases the mass of the oscillations. Hence, it increases the inertia of the system, which results in a larger time period. This is evident in the simulations presented.

The simulations reveal a maximum hydrostatic head of 2.5 MWC. However, the system design pressure is still the steady-state maximum pressure. Sustained conditions are those that remain constant over the majority of the operating time; hence, 1 MWC and 2 MWC for this system. The transients are tolerated without increasing the basic system design pressure, as long as the pressure increases does not exceed predefined limits. It is also important that the amount of time that the transient acts does not exceed a specified percentage of the total operating time. This must be considered when purchasing pressure transducers.

Following assumptions were considered:

The reservoir will have a constant water level throughout the oscillations. The inertia of the water in the surge shaft is negligible. This is valid because the kinetic energy in the water will be small compared to the hydrostatic pressure head. The kinetic energy is negligible compared to friction loss in the waterway. The changes in flowrate happens instantly. The assumption is acceptable because the valve closing time is small compared to the oscillation time of the system. The head loss during nonstationary flow is always the same as the head loss during stationary flow with the same flowrate. This is a common assumption as the frictional losses during unsteady flow is very hard to quantify (thus the reason behind this test rig). Pressure changes propagates with infinitely high velocity through the waterway. Assumed no time difference between the changes in the surge shaft water-surface and the acceleration or retardation of the water in the waterway. The elasticity of the water and conduits is of no importance. This assumption is valid because the oscillations are slow and the frequency is by no means close to the water hammer waves. Minor losses are not considered; the calculations are simplified to only consider the head loss in the waterway

7.1.2 Minimum temporal resolution

The simulations present sinusoids, which is a type of periodic functions. The frequencies in the sinusoids were: f =0.56 Hz, f =0.69 Hz, and f= 0.85 Hz.

Considering Nyquist sampling theorem the minimum sampling rate is 1.7 Hz. Which refers to the absolute minimum sampling frequency to avoid reconstructing a wrong function. However, it is recommended to operate with a temporal resolution significantly larger.

7.1.3 Water Supply

Water requirements were calculated to understand the total amount of water needed to run an experiment. Before an experiment can start, the flow has to reach steady state. When steady stat was obtained, it was estimated with 120 seconds of measurable flow. Flow situation 1 and 5, had the lowest and largest flow rates; these flow parameters form the framework for the test rig. Table 5 shows the calculated water requirements:

Table 5: Water supply requirements

	Lowest flow rate - Situation 1	**Largest flow rate - Situation 5**
Steady state flow rate, Q [litre/sec]	5	16
Time to reach steady state [sec]	23	49
Water required to reach steady state [litre]	115	784
Length of an experiment [sec]	120	120
Water in/out of the reservoir [litre]	134	310
Total water supply [litre]	**249**	**1094**

The amount of water needed complicates the idea of constructing an internal system, especially without purchasing a decent pump. It is therefore desirable to look at options using the existing components, as far as possible, to minimize the cost of realizing the project.

7.2 Final Suggestion of the Test Rig Design

7.2.1 Upper Reservoir Alt.1: Reconstruction of the Available Tank

The available tank can work as the upper reservoir. However, a reconstruction is necessary to match the requirements. Figure 14 shows a suggested reconstruction (See APPENDIX A for complete drawing).

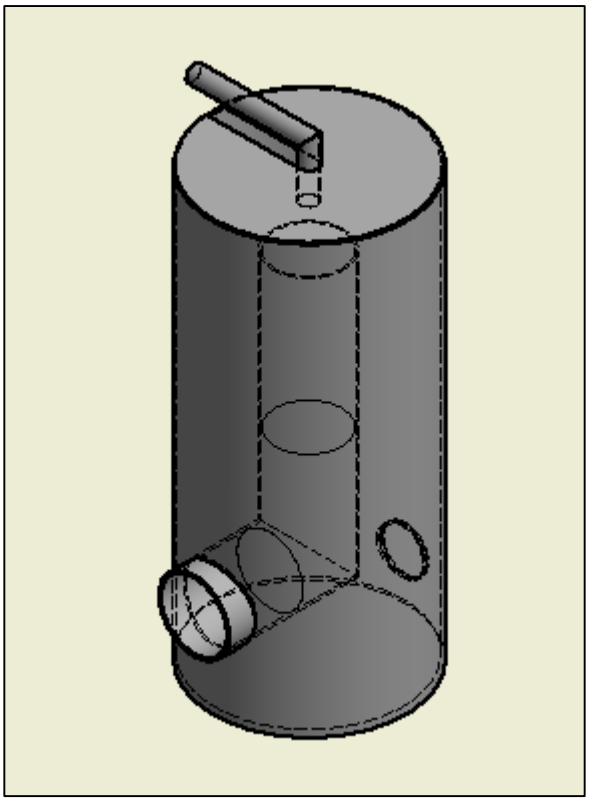

Figure 14: Drawing of the suggested tank.

Firstly, all the original components attached to the tank must be removed. Secondly, the tank must be tilted on its side to exploit its length. The tank is not designed for pressurized volume; however, in cooperation with the lab technicians it was concluded that the tank has the sufficient strength to withstand the excessive forces. The tank must be open at the top to ensure atmospheric pressure; this opening will also serve as the entrance to the tank. Thirdly, a hole for the outlet to the waterway must be made. The tank has a layer of foam insulation between the inner and outer layer. The foam is a challenging material to work with. Thus, the laboratory workers prefer to avoid unnecessary work with this layer. However, this is

unavoidable as it is necessary to make a hole for the entrance to the waterway. The entrance should be located at a certain distance above the bottom to reduce minor losses.

A cover on the top of the tank should be made to avoid water spill from the tank. This can for instance be the original top. In that case, it must be easily removable and have an opening to ensure atmospheric pressure.

Spillway

The foam insulation is the main reason for construction of an internal spillway. Another reason is that an internal spillway can be lead out through the existing manhole on the tank. The manhole (see Figure 9) is a weak spot and requires modifications to withstand the hydrostatic forces. A solution is to weld the spillway pipe to the edge of the manhole, which will strengthen this area. It is advisable to construct the spillway with stainless steel pipes. An easily adjustable spillway between one and two metres can be obtained with a threaded coupling at one metre.

The capacity of the spillway is a function of the head above the crest and the radius of the crest. The diameter of the spillway has to be sufficient to take out the excessive water. Contrary, the diameter should be as small as possible to minimize the volume it occupies. Allowing for 50 mm head above the crest and a crest radius of 150 mm gives a spillway capacity of 26 litres per second. The dimensions of the spillway can be reduced if the regulating abilities of the supply water is sufficient.

The manhole has a diameter of 460 mm, which is the spillway diameter illustrated in the drawing. However, this can be reduced with a conical connector to equal the recommended spillway diameter of 300 mm. There will be large forces acting on the spillway. The height of the inner pipe will work as a moment arm and create a torque. It is therefore necessary to install a support bracket on the opposite side of the spillway outlet, at 1- and 2-metres. The support bracket must withstand this moment force. It is also necessary to construct a support bracket at the bottom of the bend.

Water supply inlet

Advisably, the inlet pipe should be lead above the top of the tank. The kinetic energy of the water may contribute to pressure variations in the tank, which makes it essential to dissipate the energy of this water before it hits the surface. A practical solution is to connect a trajectory bucket to the end of the inlet pipe. The bucket changes the direction of the flow and flushes it towards the walls of the reservoir. Similar to the reversing buckets seen on jet skis. The bucket should be constructed or purchased with a size that matches the spillway pipe. It is important to avoid supply water to fall straight into the spillway.

An example of a trajectory bucket that dissipates the kinetic energy (Figure 15):

Figure 15: Wooldridge reverse bucket (Wooldridge Boats, 2011)

Weight

The tank itself has a weight of 580 kg and can hold 2500 litres of water in its original form. The weight changes to some extent after its reconstruction. The total weight of the tank will roughly be 3000 kg.

7.2.2 Upper Reservoir Alt.2: Construction of a New Reservoir

Construction of a new upper reservoir allows for a design precisely for its use. A suggestion of an upper reservoir is shown in Figure 16 (See APPENDIX B for a complete drawing).

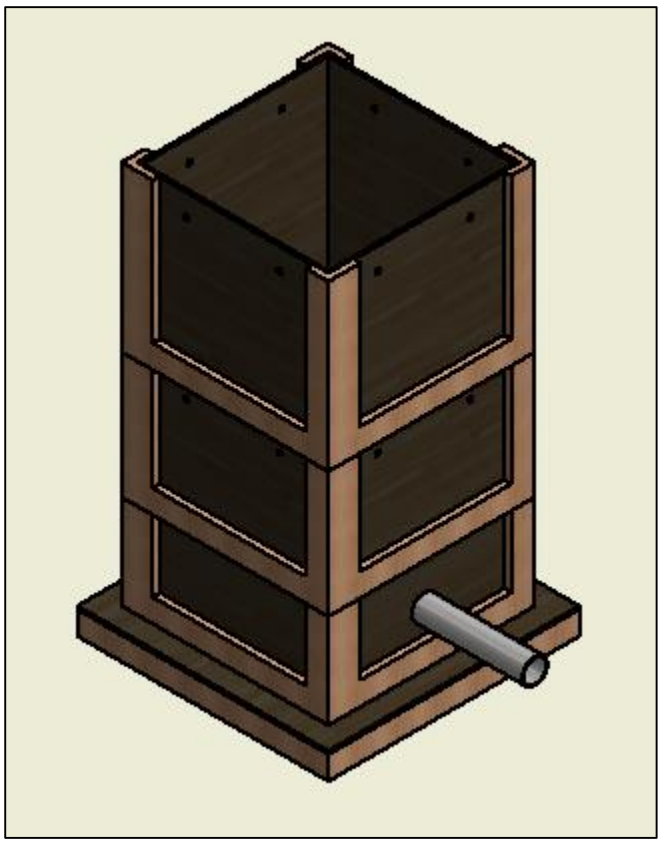

Figure 16: Drawing of the suggested new reservoir, with the supply water pipe.

Plywood plates are an appropriate material for this kind of use. Advantages using plywood is its ability to withstand stretching, shrinking and torsion. However, plywood is not waterproof and it is therefore necessary to coat the plates with fiberglass.

Considering the available space in the laboratory and the standard size of the material, an ideal reservoir is found to have a length, a width and a height of: 1220 mm, 1220 mm and 2440 mm.

With these dimensions, the walls can be made coherent without any splices. The water exposes the bottom part of the construction to high pressure. It is therefore important to construct supporting beams around the tank to withstand these forces.

Spillway

External spillways are preferred, as they do not affect the volume of the reservoir. It is recommended to have several smaller spillways to obtain a more exact water level.

A circular spillway with a crest head of 55 mm and a diameter of 32 mm has a capacity of 2.5 l/s. The construction of two circular spillways at each wall gives a total spillway capacity of 20 l/s. The drainage water can easily be lead away using standard drain hosts. Advisably, the hosts will be lead to a common discharge pipe connected to the sump in the basement of the laboratory.

To have an adjustable spillway, the circular spillways at one metre must be sealed while running experiments with two metres water column. An effective method is to plug the spillways from the inside. In that way, the hydrostatic pressure will ensure a sealed plug. Plumbers test plugs are suitable, as they are made to seal of pipes when testing drainage and pipelines. They are cheap and available in regular supply stores for plumbing equipment.

Supply water inlet

It is recommended to mount the supply water pipe to the bottom of the tank, to avoid any additional pressure variations to the water surface. Preferably, the pipe diameter should be large to reduce the kinetic energy of the supply water.

Weight

The tank can hold 3600 litres and including the weight of the material, the total weight will be roughly 4000 kg.

7.2.3 Comparison of the Upper Reservoir Alternatives

The reason to design an alternative is the need for a larger and less complicated upper reservoir. The water supply requirements are independent of the reservoir characteristics. However, the head difference is a function of the cross section area. Despite the relatively small differences in the reservoirs cross section area, it still results in significantly less impact to the head.

Table 6: Head loss

	Alt 1: available tank	**Alt 2: new reservoir**
Cross-section area [m^2]	1.15	1.44
Head reduction to reach steady state [m] – water required 0.80 m^3	0.70	0.55
Head reduction during an experiment [m] – water required 0.30 m^3	0.30	0.21

A larger reservoir ensures less circulation of the stagnant water, which means less impact on the flow. The new reservoir has the advantage of having external spillways that does not affect the volume and that are easily constructed. The supply pipe in alternative 1 are dependent on an arrangement to dissipate the energy, while this is easily solved in alternative 2. These aspects make it beneficial to construct a new reservoir. Nonetheless, the cost this implies is a decisive factor.

7.2.4 Location of the Upper Reservoir

The best location of the upper reservoir is next to the tee junction shown in Figure 12. Most importantly because this location will allow for a straight horizontal waterway. Secondly, it gives the longest possible waterway in the laboratory. This equals roughly 29 metres. Thirdly, the floor at this location only needs a small modification to carry the respective load of the reservoir. In cooperation with the lab technicians, it was concluded that a supporting pillar would give the floor the required strength. Finally, the location is right next to the recommended connection point for the supply water.

7.2.5 Surge shaft

The surge shaft characteristic should be as simple as possible, as this will ease the work of verifying the impact factors on the water flow. The characteristic of the surge shaft is recommended to be similar to a traditional shaft, constructed as a vertical pipe with a free water surface. The height is limited to 2.5 metres, due to the traversing crane in the laboratory. The surge shaft should be connected to the waterway with a tee junction, which can easily be dissembled if there is a desire to replace the traditional surge shaft.

The steel grid at the end of the laboratory have the required space to locate the surge shaft. The red circle marked on Figure 17 indicates the suggested location. The black line designates the path of the waterway. Due to the incoherent floor and the restricted space available, there are only two other locations suitable for the surge shaft. These locations are at a distance of 11 metres and 18 metres from the designated area of the upper reservoir.

7.2.6 Waterway

As previously stated, construction of the waterway is planned with the purchased stainless steel pipes, with a diameter of 150 mm. The waterway will form a horizontal line from the upper reservoir, through the tee junction forming the surge shaft and will end downstream the control valve.

The waterway must run close to the ground to make the most of the three metres height available. On the other hand, a certain distance is required due to the outlet of the waterway from the upper reservoir. A suggested distance from the floor to the waterway is set to 0.5 metre.

Depending on the measurement technique applied, access from both sides of the pipe may be required. The waterway will therefore be located at a certain distance from the wall, illustrated with the circular mark at Figure 17. Advisably, the waterway should be constructed with different pipe lengths between the flanges, to allow for an adjustable length between the upper reservoir and the surge shaft.

Figure 17: Suggested location of the surge shaft.

7.2.7 Minor losses

Some simple adjustments of the above mentioned design reduces the minor losses significantly. The recommended adjustments are elaborated here:

- The entrance of the waterway (outlet of tank) should be flush mounted with a rounded edge. To obtain the minimum loss coefficient of 0.03, the rounding ratio r/d must be equal to one or less. With an inlet pipe diameter of 300 mm, a rounding radius of at least 300 mm is required.
- It is advisable to have a conical connector as the inlet section to the waterway. Recommended dimensions are 300 mm longitudinal and width diameters of: d_1 = 150 mm, d_2 = 300 mm.
- The tee junction forming the surge shaft should be constructed with rounded edges. To obtain 90 % of the benefit of rounding it is required with a rounding ratio of 0.3. The surge shaft pipe has a diameter of 150 mm, which results in a rounding radius of 45 mm.

Piping joints

Joint design and selection can have a major impact on the performance of the piping system, the effect of minor losses and the ease of disassembly and reassembly of the test rig. The test rig design aims to be flexible and to have a piping system that contributes minimal losses. To meet these specifications, it is advisable to use flanged joints.

7.2.8 Supply Water

The best alternative for the supply of water is through the Pelton loop. The pump connected to the Pelton loop has the necessary power to provide the maximum flow rate required. It is an independent loop, which means that it is not in use by the main system. The Pelton loop has a tee junction close to the designated area for the upper reservoir, which constitutes an excellent connection point. The tee junction is shown in Figure 18.

It is recommended to replace the tee junction with a cross junction. The additional branch in the cross junction can be connected to the upper reservoir.

Figure 18: Tee junction in the Pelton-loop. The pipe on the left hand side is connected to the pump at ground level, while the pipe to the right is connected to the nozzle on the Pelton turbine. The vertical pipe leads down to the weighing tank; this is only in use when calibrating. The pipes in the tee junction have a diameter of 100 mm.

7.2.9 Flow Management

The selection of a control valve depends on the flow rates in the system, the throttling required, size and its shut off capacity. The pipe size, which in this case is 150 mm, indicates the valve size. Having a flanged valve end connection is preferred as this eases disassembly and reassembly. A needle valve meets the requirements to work as both a regulating valve and provides the necessary shut off effects. Needle valves are also appropriate for small flow rates and is therefore suitable as a control valve for this test rig. To achieve the desired flow control, a pneumatically operated, computer controlled actuator is preferable. Pressurized air at six bar is available in the laboratory as energy source for the actuator.

Ball valves contributes a very low pressure drop in open position, and have good shut-off characteristics. Additionally, ball valves availability and low price makes them a good and suitable alternative to use on drainage pipes and to separate the apparatuses to ensure a safety operation.

The upper reservoir requires a level sensor. The supply of water and the spillway will ensure a fairly accurate water level at all times. However, small pressure variation will occur. To measure these pressure variations, it is preferable to have a static pressure transducer installed at the bottom of the tank.

7.3 Final Suggestion of the Test Section

7.3.1 Measurement of Pressure

Table 7: Recommended set up and requirements of pressure measurements

Measurement of	Total pressure	Wall pressure fluctuations
Type of transducer	Static differential pressure transducer, with pizoresistive or capacitive sensing.	Miniature or MEMS pressure transducers.
Pressure level	0.3 bar	0.3 bar
Frequency response	50 -70 Hz	100 - 200 Hz
Accuracy	+/- 0.04% full scale	+/- 0.04% full scale
Electrical output	4-20 mA or 2-10 V	4-20 mA or 2-10 V
Connection	Cavity mounted	Flush mounted
Number of sensors	2 - 5	2 - 4
Placement of sensors	Along the pipe	Cross section

7.3.2 Measurement of Flow Rate and Mean Velocity

The available ultrasonic flow meter will be installed to measure the flow rate. It is advisable to place the flow meter close to the upper reservoir to minimize the response time of the respective flow rate. On the other hand, the distance must be long enough to ensure fully developed velocity profiles. The ultrasonic flow meter should not interfere with pressure measurements and it is therefore ideal to place it upstream the pressure taps.

7.3.3 Measurement of Local Flow Velocity

Alternative 1: PIV test section

Firstly, the pipe section in the test section must be replaced with a thin transparent pipe. Secondly, a rectangular pool must cover the transparent pipe, to minimize the optical aberrations. If SPIV is of interest, it is advisable to implement water filled prisms as illustrated in Figure 21 and Figure 22.

The use of PIV requires a precise calibration. A common approach is to use planar calibration targets placed coincident with the light sheet plane. The calibration target typically consists of a precise grid of markers, for instance, spaced lattice of dots printed on a transparent sheet. The calibration target has to be in the pipe section when calibrating, and it is therefore beneficial to make the sheet into a solid construction that is easy to handle. A recommended approach is to glue a thick glass plate on each side of the sheet. These glass plates can be hold in position by a bracket made of transparent sheet rolled into a cylinder, held in place by a plastic rod. See an example in Figure 19.

Figure 19: A calibration grid and its bracket made by Doorne & Hendrik (2004).

Only a small change to the test section will make the calibration useless; it is therefore important that the test section will be in a fixed position. A way to place the calibration target is to dissemble the following pipe section.

PIV set up:

In standard PIV, the camera and laser is positioned 90° relative to each other.

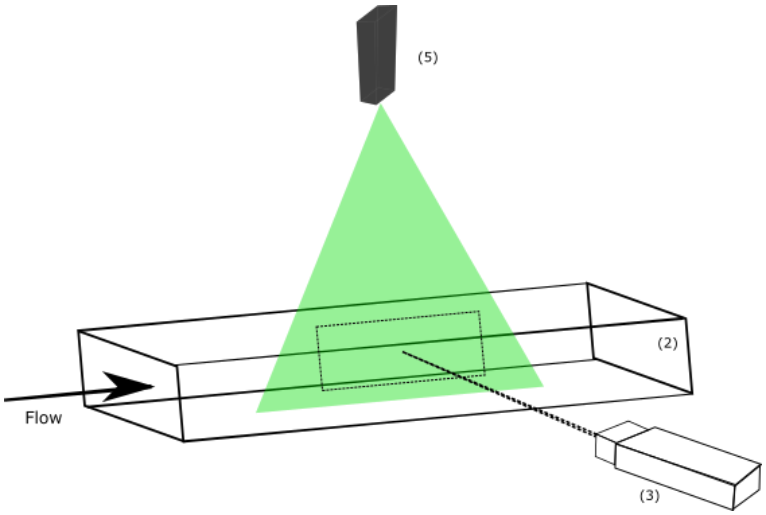

Figure 20: Standard PIV set up

Figure 21 shows a set up for measuring X – Z components using SPIV.

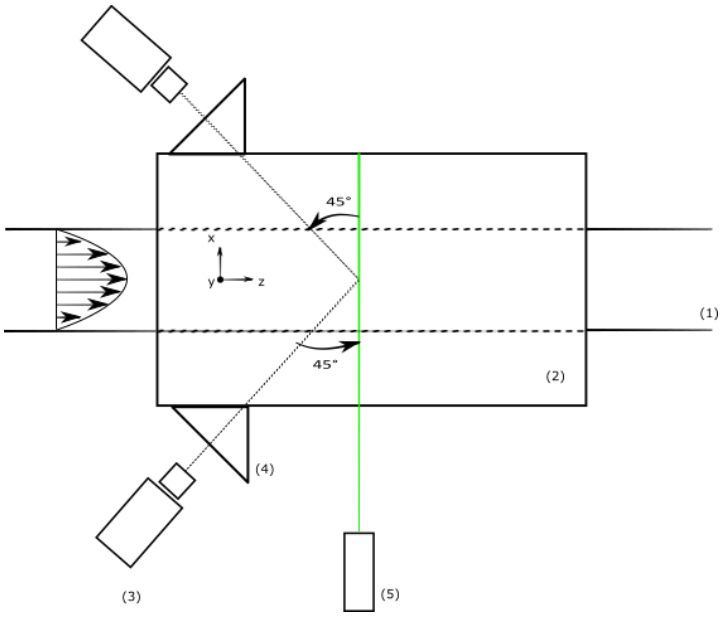

Figure 21: SPIV set up for measuring X - Z components

Figure 22 shows a set up for measuring X – Y components using SPIV.

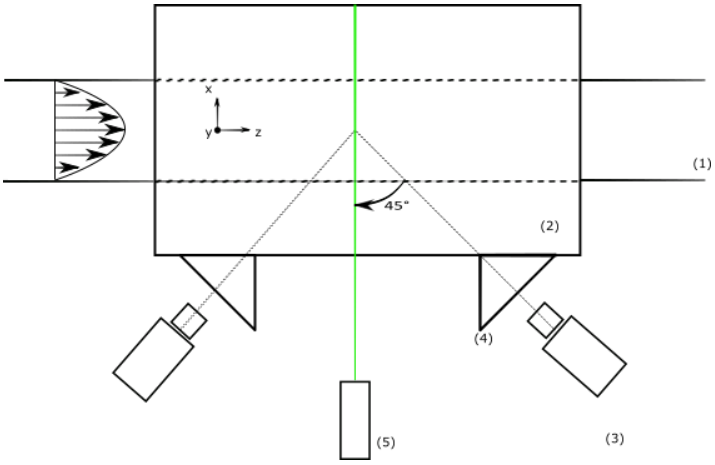

Figure 22: SPIV set up for measuring X - Y components

The numbers on the presented figures indicates the following components:

(1) Transparent pipe
(2) Rectangular water filled cover
(3) Camera
(4) External water prism
(5) Laser

The illustrations show that PIV measurements requires access from above and from both sides of the pipe. The exact distance necessary around the pipe depends on the camera lens focal length. It is common practice to apply a mirror to direct the light if there is limited space available for a camera or a laser.

Alternative 2: LDA test section

LDA measurements in circular pipes can only measure one component at a time. Measurement of axial velocities requires the optical plane to be parallel to the pipe axis. Measurement of tangential velocities requires the optical plane perpendicular to the pipe axis. There are traverse boards produced specifically for this purpose. Each LDA head position, determines a position of a measurement volume in the flow. Traversing the LDA head vertically will allow for both axial and tangential velocity components. Traversing the LDA head horizontally will allow for shift of measuring volumes along the specific axis.

The available standoff distance between the planned measurement position and the transmitting or receiving optics will directly influence the choice of front lens focal length. The design of a one-velocity component system must be rotatable about the optical axis to allow for consecutive measurements of different velocity components at the same position in the flow field. This will require transparency and a flat, vertical wall on all sides of the pipe. If consecutive measurements are of interest, a similar test section as recommended for PIV will be suitable. If only one component measurement is of interest within a region of the pipe, it can be adequate with one vertical transparent side.

7.3.4 Location of the Test Section

It is highly desirable to have the test section for local velocity measurements in the midpoint of the waterway. This will ensure fully developed velocity profiles, as both the upper reservoir and the surge shaft will form an entrance length. However, the test section for local velocities is dependent on floor underneath to locate the measurement equipment. A suitable location is along the floor in Figure 23. The waterway will be in the same direction as the large horizontal pipe. A test section located at the left hand side of the floor shown, will give a length of roughly 18 meters between the upper reservoir and the test section, and roughly 11 meters between the test section and the surge shaft.

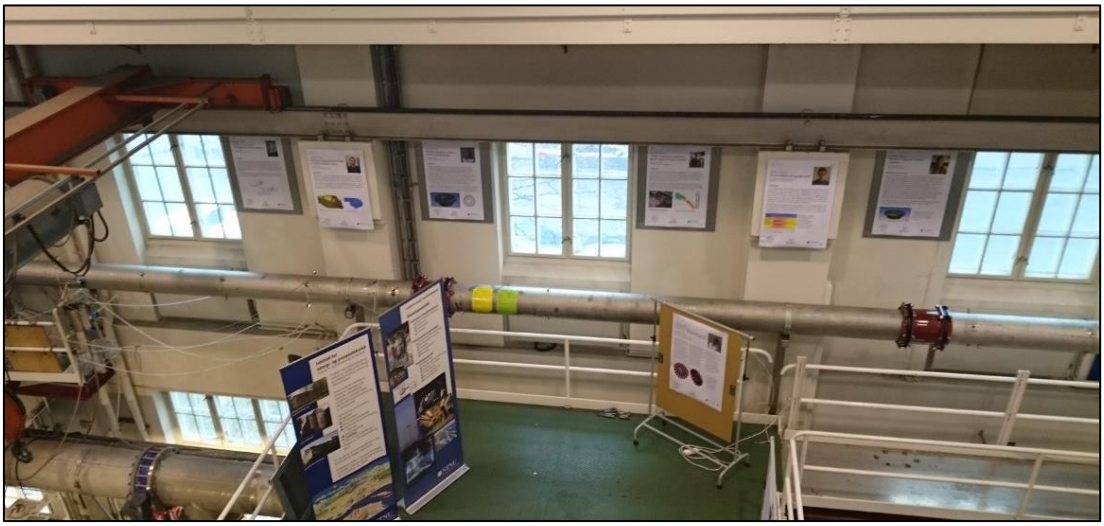

Figure 23: Suitable location of test section.

The pressure transducers are mounted to the pipe and are not dependent on having a floor underneath. Differential pressure measurements should not be conducted along the test section for local velocities. The pipe in that section will be of a different material; hence, a different surface roughness. To measure head loss along two different pipe materials will make it hard to quantify the parameters influencing the flow.

7.4 Measurement Techniques

The different measurement techniques have their clear advantages and disadvantages, which makes them suitable to specific fields of interest.

Table 8 specifies the fields of interest for the test rig and specifies a recommended measuring technique. The parenthesis symbolizes that it is feasible, but highly complex to carry out.

Table 8: Fields of interest and recommended measurement techniques

Field of interest	**Recommended measurement technique**
Static pressure/ Slow pressure fluctuations	Static pressure transducers
Pressure fluctuations	Dynamic pressure transducers or MEMS/ miniature static pressure transducer
Mean velocity	Ultrasonic flow meter (PIV)
Velocity profile	PIV • Identify flow pattern, flow separation and relative eddies
Velocity fluctuations	PIV – cross section measurements • Axial velocities • Tangential velocities • Radial velocity (reconstructed using formula) LDA – single point measurements • Axial velocities • Tangential velocities • (Radial velocities)
Wall shear stress	LDA
Two velocity components	PIV
All three velocity components	(PIV)

In contact with VIDIX – Visible Dynamics AB it came clear that CTA is not only incapable of measuring reversing flow fluctuation; flow reversal is actually damaging to the CTA sensor. The CTA can measure correctly in a conical circle from ahead. When the flow reverses, the sensor itself creates turbulence on the small films. In worst case, this will break the film sensor. This makes CTA unsuitable as a measuring technique for this test rig (Herbert, 2016, pers. Comm., 28. April).

Both the optical measurement techniques, PIV & LDA, have limited response near the wall. This is mainly due to the hydrodynamic interactions between the particles and the wall, which prevents the particles from traveling close to the wall. In some application, it is also a challenge with the background reflection from the wall that tends to overshadow particle image in the near wall region.

Experiences show that it is problematic to conduct LDA measurements of the centre area in circular pipes. Within a depth of about 1/3 of the pipe diameter, both signal strength and quality drops down. The reason is related to the optical aberration in the receiving optics. With refractive index matching experience show good results to a depth of 2/3 of the pipe diameter. A solution is to perform additional measurements from the opposite side by rotating the LDA head 180° around the pipe axis. This will result in complete distribution of each velocity component across the pipe.

A LDA set up with forward scatter mode is beneficial when investigating transient flow, as this mode allows for high data rates. This mode of operation might be challenging due to the space required to place a separate optical receiver as well as the realignment of the measurement volume will be time consuming.

It is feasible to measure radial velocities using LDA. However, it is a highly complex process. The two major problems are: how can measurement volume be accurately positioned and orientated? How can beam intersection angle be calculated? There are theories how to solve these problems, but there is no known reference experiment. Therefore, the measurements of radial velocities using LDA would by highly experimental.

Stereo PIV is the only measurement technique considered that can measure a complete set of velocity components on this facility. A four beam LDA is not feasible in circular pipe and CTA is no longer an option due to reversing flow. However, the SPIV only measures the out of plane vector indirectly. The three-component vector is seen from two different directions

and reconstructed using formulas. The optical distortion, image light sheet misalignment, camera viewing angles and the image reconstruction are challenges that makes the three component SPIV a highly complex measurement technique.

8 Conclusion

The first step towards the establishment of a test rig in the Water Power Laboratory is completed. The possible dynamic flow situations are identified and simulated.

The results point out the possibilities and limitations in the laboratory. The most decisive findings are the three metres height limitation, supply water alternatives and the suitable location of the test rig in the laboratory.

The study of relevant measurement techniques discovered that Particle Image Velocimetry and Laser Doppler Anemometer are both suitable to measure local velocities in the test rig. A thorough review has mapped their advantages and disadvantages. The study shows that static pressure transducers have the required temporal resolution to capture the slow oscillations of the possible flow fields. Contrary, the study revealed that hot-wire measurements are not applicable for this test rig.

Further Work

Natural successor from where this thesis ends:

Second stage:

After the completion of the first stage, with drafts of calculations, the design processes to the second stage. The second stage normally consist of detailed physical design of the piping system and equipment, piping stress analysis and procurement of materials. However, the design process is an iterative process; it is advisable to issue calculations at various stages of completeness, based on firmness of the design input.

- Detailed equipment drawings.
- The design and procurement of pipe supports. A detailed pipe support drawing containing the necessary fabrication details and cost of materials.
- Piping stress analyses that addresses the static and dynamic loading resulting from the effects of gravity, internal and external pressure, changes in fluid flow rate and environmental conditions.

Third stage:

When the design reaches completion and the remaining materials have been purchased, the installation and construction of the test rig can begin.

Suggestions to extensive investigation:

- Optical measuring techniques in circular pipes are challenging due to the optical aberrations. It would be interesting to study and investigate the possibility to optimize a test section for optical measurements.
- Study of the behaviour of the amplitude in the surge shaft.
- Detailed calibration plan for SPIV

Bibliography

Bagheri, A., et al. "Hydraulic Evaluation of the Flow over Polyhedral Morning Glory Spillways." *World Applied Sciences Journal* 9.7 (2010): 712-717.

Brunone, Bruno, et al. "Velocity profiles and unsteady pipe friction in transient flow." *Journal of water resources planning and management* 126.4 (2000): 236-244.

Çarpinlioğlu, Melda Özdinç, and Mehmet Yaşar Gündoğdu. "A critical review on pulsatile pipe flow studies directing towards future research topics." *Flow Measurement and Instrumentation* 12.3 (2001): 163-174.

Cengel, A.C, Cimbala J.M. (2014) "*Fluid mechanics"*. Singapore: Mc Graw Hill.

Chaudhry, M. H. (1979). "*Applied hydraulic transients".* (No. 627 C4). New York: Van Nostrand Reinhold.

Dantec Dynamics (2013) *"Measurement principle of LDA".* [Internet] Available at: <http://www.dantecdynamics.com/measurement-principles-of-lda>

David M. Eckmann and James B. Grotberg (1991). "*Experiments on transition to turbulence in oscillatory pipe flow"*. Journal of Fluid Mechanics, 222, pp 329-350 doi: 10.1017/S002211209100112X

Durst, F., J. Jovanovic, and J. Sender. "*LDA measurements in the near-wall region of a turbulent pipe flow*." Journal of Fluid Mechanics 295 (1995): 305-335.

Eckmann, David M., and James B. Grotberg. "*Experiments on transition to turbulence in oscillatory pipe flow." Journal of Fluid Mechanics* 222 (1991): 329-350.

Guttormsen, O. (2013) "*Vassdragsteknikk 2"*. Trondheim: NTNU

He, S., and J. D. Jackson. "*A study of turbulence under conditions of transient flow in a pipe*." Journal of Fluid Mechanics 408 (2000): 1-38.

Hino, Mikio, Masaki Sawamoto, and Shuji Takasu. "*Experiments on transition to turbulence in an oscillatory pipe flow."* Journal of Fluid Mechanics 75.02 (1976): 193-207.

Idelchik, I. E., & Fried, E. (1986). "*Handbook of hydraulic resistance"*.

Iguchi, M. Ohmi, M. and Maegawa, K. (1982) *"Analysis of free oscillating flow in a U-shaped Tube"*. [Internet] Available at: <https://www.jstage.jst.go.jp/article/jsme1958/25/207/25_207_1398/_pdf>

Jensen, Kim D. "*Flow measurements*." Journal of the Brazilian Society of Mechanical Sciences and Engineering 26.4 (2004): 400-419.

Jørgensen, Finn E. (2002) "*How to measure turbulence with hot-wire anemometers*". [Internet] Available at:< http://web.iitd.ac.in/~pmvs/courses/mel705/hotwire2.pdf>

Landteknikk, 2005. "Gårdstank". [Image online] Available at: <http://www.skalafabrikk.no/var/ezwebin_site/storage/original/application/943e3711c7814e6893ed9fbeae7d10b7.pdf> [Accessed 16.02.2016].

Lodahl, C. R., B. Mutlu Sumer, and Jørgen Fredsøe. "*Turbulent combined oscillatory flow and current in a pipe*." Journal of Fluid Mechanics 373.25 (1998): 313-349.

Massoud, Mahmoud. "*Engineering thermofluids"*. Berlin, Germany: Springer, 2005.

Merkli, P., and H. Thomann. "*Transition to turbulence in oscillating pipe flow*." Journal of Fluid Mechanics 68.03 (1975): 567-576.

NTNU (2015) "*Water Power Laboratory"* [Internet] Available at: <https://www.ntnu.edu/ept/laboratories/waterpower >

Ohmi, M., et al. (1982). "*Transition to Turbulence and Velocity Distribution in an Oscillating Pipe Flow."* Bulletin of JSME 25(201): 365-371.

Oppenheim, Alan V., Ronald W. Schafer, and John R. Buck. *Discrete-time signal processing*. Vol. 2. Englewood Cliffs, NJ: Prentice hall, 1989.

PCT (2014) "*Pressure sensors and transmitters*" [Internet] Available at: http://www.pcb.com/linked_documents/pcb/catalog/sections/pcb_stc_0207_pressure.pdf

Raffel, M. Willert, C.E. Werley, S.T., Kompenhans, J. (2007) "*Particle Image Velocimetry"*.

Rennels, Donald C., and Hobart M. Hudson. "*Pipe Flow: A Practical and Comprehensive Guide"*. John Wiley & Sons, 2012.

Samson (2003) "*Cavitation in Control Valves*". [Internet] Available at: <https://www.samson.de/pdf_en/l351en.pdf>

Sensormag (2016) "*A Dozen Ways to Measure Fluid Level and How They Work*". Questex, LLC

Sergeev, S. I. "*Fluid oscillations in pipes at moderate Reynolds numbers.*" Fluid Dynamics 1(1): 121-122.

Seume, Joerg Reinhart (1988) "*An experimental investigation of transition in oscillating pipe flow*."

Smith, Peter (2004) "*Valve selection handbook*". Oxford: Elsevier.

Tavoularis, Stavros (2005) "*Measurement in fluid mechanics*". United States: Cambridge University Press.

Van Doorne, C. W. H., and J. Westerweel. "*Measurement of laminar, transitional and turbulent pipe flow using stereoscopic-PIV*." *Experiments in Fluids* 42.2 (2007): 259-279.

Vítkovský, J. P., et al. "*Advances in unsteady friction modelling in transient pipe flow*." VII International Conference on Pressure surges: Safe Design and Operation of Industrial Pipe Systems, 8., 2000, The Hague. Proceedings. 2000.

Wooldridge Boats (2011) "*Reversing bucket*." [Image online] Available at: <http://www.wooldridgeboats.com/store/equipment/wooldridge-reverse-bucket-w-flo-tec-linkage-> [Accessed 20.05.2016].

Zhang, Zhengji. (2010) "*LDA application methods: laser Doppler anemometry for fluid dynamics"*. Springer Science & Business Media.

Zhao, T. S., and P. Cheng. "*Experimental studies on the onset of turbulence and frictional losses in an oscillatory turbulent pipe flow." International journal of heat and fluid flow* 17.4 (1996): 356-362.

APPENDIX A

Upper reservoir alternative1:

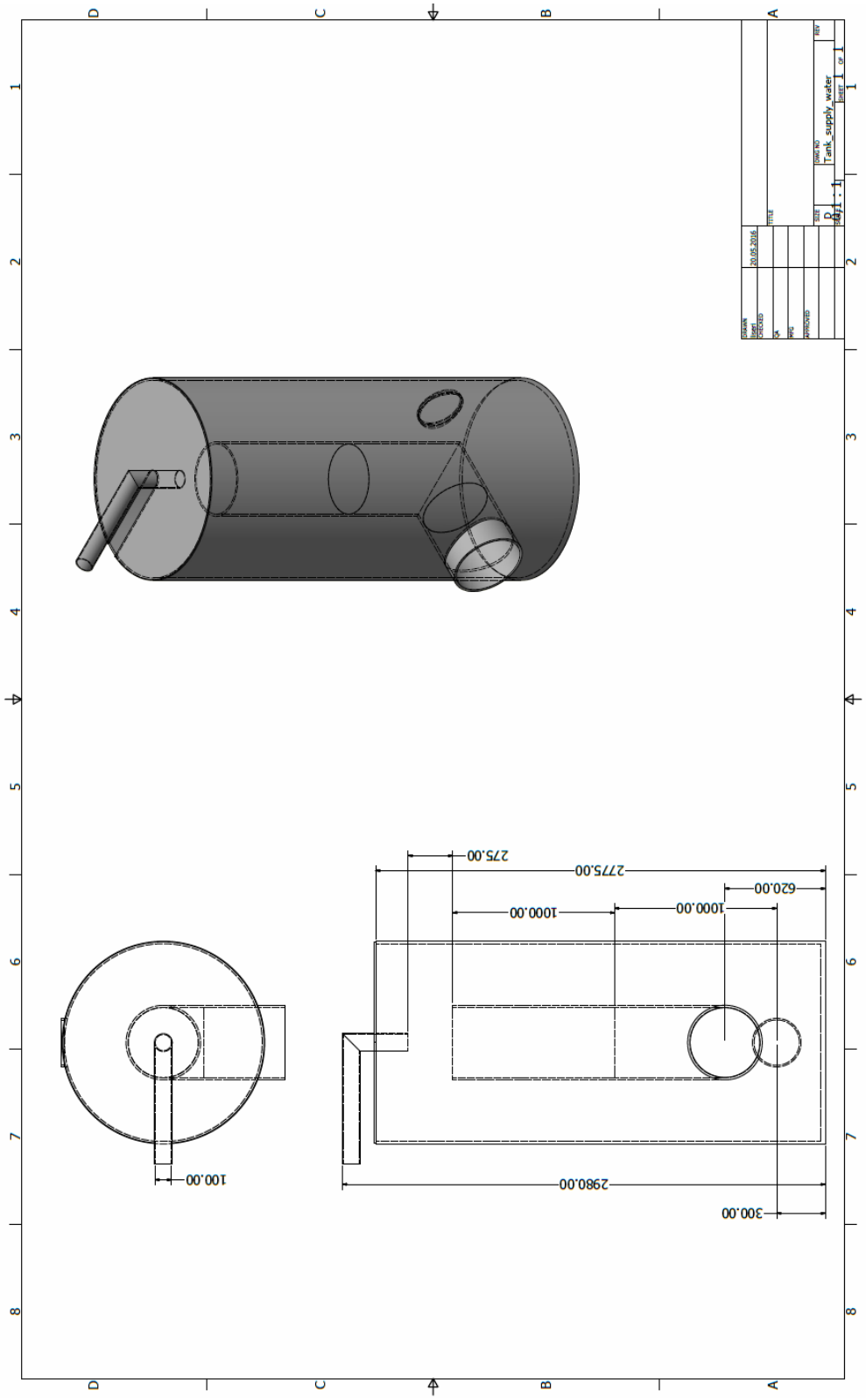

APPENDIX B

Upper reservoir alternative 2:

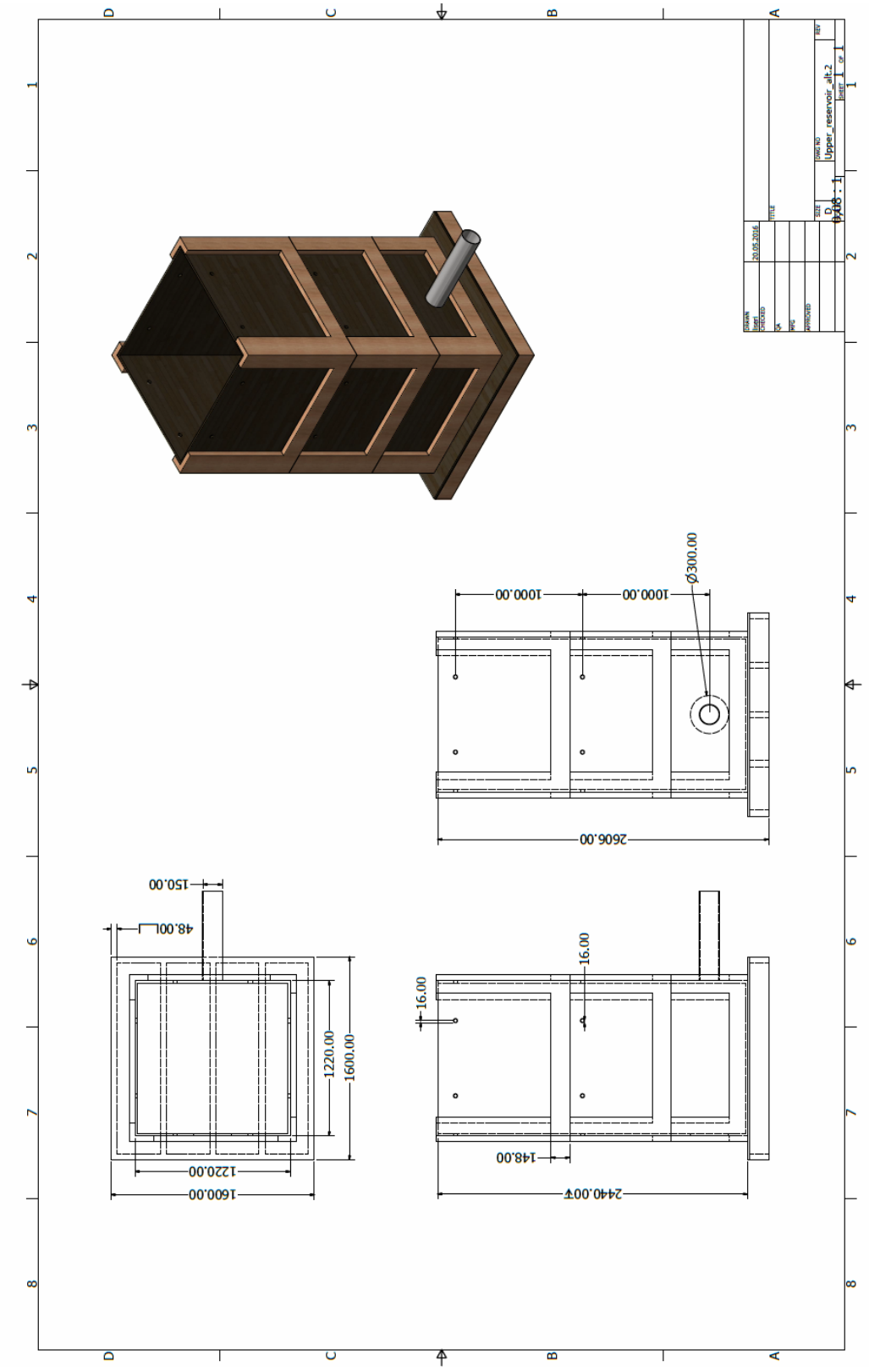

Appendix C

This appendix contains the first 20 steps of the Euler's integration method for flow situation 1. These are part of the data behind the simulated oscillations in the surge shaft.

Time	dt	dz	z	z-hf	dv	v	hf= αv^2	Water level	Reynolds number
s	s	m	m	m	m/s	m/s	m	m	
0	0	0	0,02	0	0	0,283	0,02	1,98	3,24E+04
1	1	-0,282965478	-0,26	-0,28	-0,09572039	0,187	0,00798069	2,26	2,14E+04
2	1	-0,187245087	-0,45	-0,46	-0,15559521	0,032	0,00022802	2,45	3,62E+03
3	1	-0,031649876	-0,48	-0,48	-0,16367906	-0,132	-0,00396789	2,48	1,51E+04
4	1	0,132029181	-0,35	-0,35	-0,1175974	-0,250	-0,01418409	2,35	2,86E+04
5	1	0,24962658	-0,10	-0,09	-0,02969886	-0,279	-0,01775991	2,10	3,20E+04
6	1	0,279325439	0,18	0,20	0,06599981	-0,213	-0,01035871	1,82	2,44E+04
7	1	0,213325631	0,39	0,40	0,13565907	-0,078	-0,00137305	1,61	8,89E+03
8	1	0,077666556	0,47	0,47	0,15889216	0,081	0,00150178	1,53	9,30E+03
9	1	-0,081225608	0,39	0,39	0,13044302	0,212	0,01019842	1,61	2,42E+04
10	1	-0,211668624	0,18	0,17	0,05589877	0,268	0,01629619	1,82	3,06E+04
11	1	-0,26756739	-0,09	-0,11	-0,03667555	0,231	0,01213492	2,09	2,64E+04
12	1	-0,230891837	-0,32	-0,34	-0,11337303	0,118	0,00314365	2,32	1,35E+04
13	1	-0,117518807	-0,44	-0,44	-0,15008528	-0,033	-0,00024141	2,44	3,73E+03
14	1	0,032566471	-0,41	-0,41	-0,13792374	-0,170	-0,00661635	2,41	1,95E+04
15	1	0,170490212	-0,24	-0,23	-0,07809453	-0,249	-0,01406594	2,24	2,85E+04
16	1	0,248584741	0,01	0,03	0,0085157	-0,240	-0,01311874	1,99	2,75E+04
17	1	0,240069039	0,25	0,26	0,08940485	-0,151	-0,00516702	1,75	1,73E+04
18	1	0,15066419	0,40	0,41	0,13768103	-0,013	-3,8369E-05	1,60	1,49E+03
19	1	0,012983157	0,41	0,41	0,14033802	0,127	0,00369191	1,59	1,46E+04
20	1	-0,127354866	0,29	0,28	0,09599508	0,223	0,01135511	1,71	2,56E+04